JPEDAV (2014) 35:284–313
DOI: 10.1007/s11669-014-0301-2
1547-7037 ©ASM International

Thermodynamic and Experimental Study of the Mg-Sn-Ag-In Quaternary System

Jian Wang, Pierre Hudon, Dmytro Kevorkov, Patrice Chartrand, In-Ho Jung, and Mamoun Medraj

(Submitted September 12, 2013; in revised form March 11, 2014; published online April 10, 2014)

Phase equilibria in the Mg-rich region of the Mg-Sn-Ag ternary system were determined by quenching experiments, differential scanning calorimetry, electron probe micro-analysis, and X-ray diffraction techniques. No ternary compounds were found in the studied isothermal sections. A critical evaluation of the available experimental data and a thermodynamic optimization of the Mg-Sn-Ag-In quaternary system were carried out using the calculation of phase diagrams method. The modified quasichemical model in the pair approximation was used for the liquid solution, which exhibits a high degree of short-range order. The solid phases were modeled with the compound energy formalism. All available and reliable experimental data were reproduced within experimental error limits. A self-consistent thermodynamic database was constructed for the Mg-Sn-Ag-In quaternary system, which can be used as a guide for Mg-based alloys development.

Keywords electron probe micro analyzer, Mg-based alloys, phase diagram, thermodynamic modeling

1. Introduction

Magnesium alloys, with a density around 1.74 g/cm^3 which is nearly 1.6 and 4.5 times less dense than aluminum alloys and steel, is an exceptionally lightweight structural materials. The low density of magnesium alloys is a strong driving force for their applications in the transportation industry with the associated reductions in weight of vehicles and fuel consumption. Magnesium and its alloys have some advantageous properties as high thermal conductivity, high dimensional stability, high damping characteristics, high machinability, and they are also completely recyclable,[1] which makes them suitable for automobile and computer parts, aerospace components, and household equipment parts. Up to now, several series of magnesium alloys have been developed for different applications, such as Mg-Al based, Mg-Zn based, Mg-RE based alloys. Unfortunately, most of these series have a number of undesirable properties (especially at elevated temperatures) including poor corrosion resistance, poor creep resistance, and low wear resistance, which restricts their applications. The current trend, instead, is to improve Mg-based alloys for high temperature applications. To this end, Mg-Sn based alloys are good candidates because they have stable microstructures and good mechanical properties at high temperatures due to the high solubility of Sn in hcp Mg and to the possibility to precipitate a cubic second phase (Mg_2Sn) in the magnesium-rich matrix.[2,3] Previous investigations[2-4] also indicate that Mg-Sn alloys with additional alloying elements have comparable or even better creep properties than AE42 alloys. Moreover, it is known that Sn can improve the corrosion resistance.[5,6] Unfortunately, the behavior of Mg-Sn alloys after quenching require quite long time to reach the peak hardness, which is not practical for industrial applications.[7] Hence, it is necessary to improve the age hardening response and creep resistance behavior. Adding microalloying elements such as In, Ag, Ca, Li, Na, Zn, Sr and rare-earth elements can potentially achieve this goal.[8-10] Among these, In and Ag are of interest. Mendis et al.[8,9] for example, proposed a qualitative thermo-kinetic criteria for choosing microalloying elements that can be applied to precipitation hardenable alloys. Indium was one of these elements and the authors[8,9] were able to show that additions of In + Li to Mg-Sn alloys increase the number density of precipitates by approximately one order of magnitude, resulting in 150% hardening increment.[9] In the case of Ag, its addition to Mg-Sn alloys can improve the mechanical properties,[11,12] greatly affects the grain refinement and corrosion resistance,[13,14] and bias the age hardening response which enhances the mechanical properties. Recently, Son et al.[15] also found that the addition of Ag leads to the formation of fine submicron-sized Mg-Ag particles, grain refinement, and weaker basal texture. The addition of In and Ag to Mg-Sn based alloys is thus quite beneficial.

In order to design new Mg-Sn-based alloys and to understand the relationships between their microstructures and mechanical properties, a better knowledge of the phase relations in Mg-Sn-based alloys is imperative. Obtaining

Jian Wang and **Patrice Chartrand,** Center for Research in Computational Thermochemistry (CRCT), Dept. of Chemical Engineering, École Polytechnique, Montreal, QC H3C 3A7, Canada; **Pierre Hudon** and **In-Ho Jung,** Department of Mining and Materials Engineering, McGill University, 3610 University Street, Montreal, QC H3A 0C5, Canada; and **Dmytro Kevorkov** and **Mamoun Medraj,** Department of Mechanical Engineering, Concordia University, 1455 De Maisonneuve Blvd. West, Montreal, QC H3G 1M8, Canada. Contact e-mail: patrice.chartrand@polymtl.ca.

such information by the sole mean of experimental techniques is cumbersome and costly. Fortunately, thermodynamic modeling of multi-component systems by the calculation of phase diagrams (CALPHAD)[16] approach is a very efficient way to investigate phase equilibria.[17] Coupled phase-field calculations, ab initio calculations, and physical properties modeling permit one to estimate material properties.[18] In the present work, phase relations in the Mg-rich portion of the Mg-Sn-Ag ternary system were determined and the thermodynamic optimization of Mg-Sn-Ag-In quaternary system was carried out as part of a wider thermodynamic database development project for the Mg-X (X: Ag, Ca, In, Li, Na, Sn, Sr and Zn) multi-component system.

2. Literature Review

2.1 The Ag-Mg System

The Ag-Mg system was critically reviewed by Nayeb-Hashemi and Clark.[19] There are five solid phases: fcc (Ag), hcp (Mg), bcc_B2, Ag_3Mg and $AgMg_3$ in the Ag-Mg system. The liquidus was first determined by Zemczuznyj[20] using thermal analysis; four invariant reactions: $L \leftrightarrow AgMg_3$ + hcp (Mg), $L \leftrightarrow$ bcc_B2 + fcc (Ag), $L \leftrightarrow$ bcc_B2, and L + bcc_B2 $\leftrightarrow AgMg_3$ were reported at 472, 759, 820 and 492 °C, respectively. Andrews and Hume-Rothery,[21] Payne and Haughton,[22] and Hume-Rothery and Butchers[23] determined the liquidus by thermal analysis and results are all in good agreement with each other. The $AgMg_3$ phase was first reported by Ageew and Kuznezow[24] by studying several alloys using metallographic methods and the structure was found to be hexagonal with 8 atoms per unit cell. However, results from later investigators[25-27] suggest that Mg_3Ag has a more complex structure. An X-ray diffraction analysis performed by Prokofev et al.[28] demonstrated that $AgMg_3$ appear to be constituted of ϵ (bct) at high temperature and ϵ′(fcc)at low temperature. Later, Kolesnichenko et al.[29] rather found that the phase $AgMg_4$ must be the one described earlier as $AgMg_3$; according to them, its structure is hexagonal. Kolesnichenko et al.[29] also pointed out that the structural formula of ϵ′(fcc)is $Ag_{17}Mg_{54}$. Recently, phase equilibria in the Ag-Mg system were studied by Lim et al.[30] using DSC, XRD, and scanning electron microscopy (SEM); the existence of $AgMg_4$ and $Ag_{17}Mg_{54}$ was then confirmed. The phase relations and the polymorphic transition temperature of the ordering phase Ag_3Mg (fcc_L12) were determined by Gangulee and Bever.[31]

The enthalpy of formation of the liquid phase at 1050 °C was measured by Kawakami[32] using calorimetric measurement method. The activity of Mg in the Ag-Mg liquid phase was determined by Gran et al.[33] by measuring the vapor pressure at 1300 and 1400 °C and with a gas equilibration technique at 1500 and 1600 °C. The enthalpies of formation of the bcc_B2 and fcc phases over the temperature range of 350 to 500 °C were measured by Kachi[34,35] by performing emf measurements. The enthalpy of formation of the bcc_B2 phase between 39 and 54.8 Mg (at.%) at 0 °C was measured by Robinson and Bever[36] by tin-solution calorimetry. Later, Jena and Bever[37] measured the enthalpy of formation of the bcc_B2 phase at 78, 195 and 273 K with the same equipment. The partial molar enthalpy, entropy and free Gibbs energy changes of the bcc_B2 phase were derived by Trzebiatowski and Terpilowski[38] based on their emf results. The enthalpies of formation of the fcc and Ag_3Mg phases at 0 °C were determined by Gangulee et al.[31] by solution calorimeter. All the reported results of the enthalpy of formation of solid phases are in good agreement.

2.2 The Ag-In System

Weibke and Eggers[39] investigated the phase relations in the whole Ag-In binary system by means of thermal analysis, X-ray analysis, and photomicrography. According to their experimental results, the Ag-In phase diagram is constituted of six solid phases: fcc, bcc, γ (hcp), δ (Ag_5In_2), and ε and φ ($AgIn_3$). The bcc phase is only stable in the temperature range of 660 to 667 °C and possesses a narrow solid solubility field, from 25 to 29 at.% In. Hume-Rothery et al.[40] studied the solubility limit of indium in the terminal phase of fcc (Ag) with temperature. Owen and Roberts[41] determined carefully the fcc phase boundaries below the melting point and their results are in good agreement with the ones reported by Weibke and Eggers[39] and Hume-Rothery.[40] Hellner[42] studied the crystal structure and the solubility range of the intermetallic phases with X-ray analysis and pointed out that an ordered phase, γ′ ($MgCd_3$-type), exists in Ag_3In below 187 °C. The φ ($AgIn_3$) phase reported by Weibke and Eggers[39] was confirmed as $AgIn_2$ (with a $CuAl_2$-type crystal structure) by Hellner.[42] Campbell and Wagemann[43] re-investigated the phase equilibra in the whole composition range of the Ag-In system by DTA, XRD, photomicrography and EPMA. The existence of the bcc phase was confirmed between 660 and 695 °C and the hcp phase was found to decompose at 670 °C following the peritectoid reaction fcc + bcc ↔ hcp. In the Ag-rich area below 300 °C, a primitive cubic phase,α′, was reported to exist below about 73.8 at.% Ag. The homogeneity region of the ε phase was reported to lie between 67 and 70 at.% Ag by Campbell and Wagemann.[43] Uemura and Satow[44] investigated the order-disorder transition of Ag_3In by using specific heat capacity measurements, electrical resistivity, magnetic susceptibility and X-ray analysis. The order-disorder transition of the hcp phase was observed to occur at 214 °C. Satow et al.[45] studied the phase transition of $AgIn_2$ with the help of the same techniques and found that the cubic phase transforms to the hcp one at 222 °C. Based on the experimental results of the time, Barren[46] compiled and presented a new phase diagram for the Ag-In binary system. Later, Moser et al.[47] investigated the phase relations in the Ag-In binary system by using diffusion couple measurements, DSC and metallographic methods. Their experimental results are in good agreement with previous data. Recently, Jendrzejczyk and Fitzner[48] determined the liquidus of the Ag-In binary system over whole composition range using emf measurements.

The heat of formation of the solid and liquid alloys of the Ag-In system at 450 °C were measured by Kleppa[49] using calorimetric measurements. Prezdziecka-Mycielska et al.[50] and Nozaki et al.[51] derived the partial and integral values of excess enthalpy, excess free Gibbs energy and excess entropy of liquid Ag-In alloys at 727 and 827 °C based on the emf measurements results. Beja[52] determined the enthalpy mixing of the liquid phase at 755 °C using calorimetric measurements method. Itagaki and Yazawa[53] measured the heat of mixing at 970 °C in Ag-In liquid alloys by adiabatic calorimetry; the minimum value recorded was −4.54 kJ/mol-atom at 66 Ag at.%. Alcock et al.[54] and Qi et al.[55] derived the enthalpy of mixing, Gibbs energy of mixing and entropy of mixing of liquid Ag-In alloys at 1027 °C based on the results of vapor pressure measurements with the Knudsen cell and mass spectrometer. Their results are in good agreement with previous works. The activity of In in the liquid phase at 777, 800, and 977 °C were determined by Kameda et al.[56] from emf measurements. The integral molar enthalpy of liquid Ag-In at 470 and 1007 °C were measured by Castanet et al.[57] by drop calorimetry. Recently, Jendrzejczyk and Fitzner[48] derived the activities, Gibbs energy of mixing and enthalpy of mixing of liquid Ag-In alloys based emf measurements using solid oxide galvanic cells with zirconia electrolyte. The heat of formation of the fcc phase at 44 °C was measured by Orr and Hultgren[58] by means of calorimetric measurements method. The activity of In in the fcc phase at 727 °C was measured by Masson and Pradhan[59] with vapor pressure measurement method.

2.3 Ag-Sn System

The liquidus of the Ag-Sn binary system was determined by Heycock and Neville[60-62] by employing samples prepared in heavy iron blocks covered by paraffin, to prevent the oxidation of tin, and by thermal analysis. Peternko[63] investigated the system with thermal analysis and metallographic methods and reported the existence of a new intermetallic compound, Ag_3Sn, with a peritectic melting temperature of 480 °C following the reaction liquid + fcc ↔ Ag_3Sn. Puschin[64] studied molten Ag-Sn alloys with the emf method and observed the existence of a new phase, named ζ (Ag_6Sn or Ag_5Sn), in the Ag-rich region. Murphy[65] investigated the whole Ag-Sn system with thermal analysis and metallographic methods and determined the solid solubility boundaries of the fcc, ζ and Ag_3Sn phases. Murphy[65] also found that the solid solubility of Ag in the terminal bct (Sn) phase was less than 0.1 at.% Ag at 206 °C. Hume-Rothery et al.[66] and Hume-Rothery and Eutchers[67] determined the liquidus of the Ag-Sn binary system by thermal analysis; their results are in good agreement with previous investigations.[60-63] Hanson et al.[68] employed thermal analysis and carefully determined the liquidus between 0 to 6 at.% Ag. The eutectic liquid ↔ Ag_3Sn + bct (Sn) was located at 3.5 at.% Ag and 221 °C. The solid solubility of fcc was determined by Owen and Roberts[69] with XRD; their results are in good agreement with the previous work of Murphy.[65] Umansky[70] re-investigated the whole Ag-Sn system with XRD and confirmed the existence of the fcc, ζ and Ag_3Sn phases. The solid solubility range of the fcc phase was also measured. The solubility of Ag in the terminal phase bct (Sn) was determined by Vnuk et al.[71] with the help of hardness measurements on several heat treated alloys, and the maximum solid solubility of Ag in bct (Sn) was found to be 0.09 at.% Ag at the eutectic temperature of 221 °C. All the available experimental phase equilibria data of the Ag-Sn binary system were compiled by Karakay and Thompson.[72]

Frantik and McDonald[73] derived the activity, partial molar Gibbs energy and integral Gibbs energy of molten Ag-Sn alloys based on their experimental data obtained by emf measurements method. Yanko et al.[74] studied the activity of dilute Ag-Sn liquid solutions with the emf method in the temperature range of 250 to 412 °C. Both of their results were shown that the Ag-Sn solution is not an ideal mixing solution. Kleppa[75] measured the enthalpy of formation of solid and liquid Ag-Sn phases at 450 °C using calorimetric measurement method. The positive enthalpy of mixing of Ag-Sn liquid solution was determined in the composition range from 0 to 40 at.% Ag at 450 °C, which is in agreement with the derived data by Frantik and McDonald[73] Nozaki et al.[76] derived the partial and integral molar excess Gibbs energy, excess entropy and excess enthalpy of molten Ag-Sn alloys based on the experimental data obtained using emf measurements method, and the activity of Sn in the liquid phase at 827 °C was reported in their work. Elliott and Lemons[77] determined the activity of Ag and Sn in the dilute Ag-Sn liquid solution using emf measurements method. Itagaki and Yazawa[53] measured the enthalpy of mixing of the liquid phase in Ag-Sn alloys at 970 °C using adiabatic calorimetry. An "N" type enthalpy of mixing with the positive value part in the composition range from 0 to 50 Ag (at.%) and negative part with a minimum value of −2777 J/mol-atom at 76.4 at.% Ag were reported in their work, which are in good agreement with the previous one reported by Kleppa[75] Castanet and Laffitte[78] reoprted the enthalpy of mixing of Ag-Sn liquid phase at 1007 °C using calorimetric measurements method, which are in agreement with the data reported by Itagaki and Yazawa[53] and Kleppa[75] Chowdhury and Ghosh[79] derived the activity of Sn and Ag in liquid phase in the composition range from 20 to 90 Sn (at.%) in the temperature range of 552 to 838 °C using emf measurements method. The reported activity of Sn in liquid solution at 627 °C are in good agreement with the data reported by Frantik and McDonald[73] Okajima and Sakao[80] reported the activity of Ag in the liquid phase at 500, 560 and 620 °C using emf measurements method. The activity of Sn in the liquid phase at 827 and 727 °C were determined by Iwase et al.[81] using the emf measurements method with two different solid-oxide galvanic cells. And the derived activity of Sn in liquid solution in the work of Iwase et al.[81] are self-consistent, but are not in agreement with the previous reported results[73,79,80] The activity of Sn in the liquid phase at 600 and 700 °C were measured by Kameda et al.[82] using the emf measurements method. The enthalpy of formation of solid phases were measured by Flandorfer et al.[83] with calorimetric measurements method.

Table 1 Thermodynamic optimization status of sub-systems of Mg-Sn-Ag-In quaternary system

System	Reference	
	BW for liquid solution	MQMPA for liquid solution
Ag-Mg	Lim et al.[30]	N/A
Ag-In	Moser et al.[47], Liu et al.[91]	N/A
Ag-Sn	Oh et al.[98]	N/A
In-Mg	N/A	Wang et al.[97]
In-Sn	Liu et al.[91]	Wang et al.[97]
Mg-Sn	Meng et al.[99]	Jung et al.[95,96]
Mg-Sn-Ag	N/A	N/A
Mg-Sn-In	N/A	Wang et al.[97]
Mg-Ag-In	N/A	N/A
Sn-Ag-In	Liu et al.[91]	N/A

BW: Bragg-Willams model, MQMPA: Modified quasichemical model in the pair approximation

Rakotomavo et al.[84] studied the enthalpy of mixing of liquid phase at 1100 °C with calorimetric measurements method. Laurie et al.[85] reported the partial enthalpy mixing of Ag-Sn liquid phase at 554 °C using emf measurement and calorimetric measurement methods. The activity of Ag and Sn in liquid phase and partial moral enthalpy of the Ag-Sn liquid phase were derived by Yamaji and Kato[86] based on their experimental data obtained by using emf measurements method and mass spectrometer measurements, which are in agreement with the reported data from Iwase et al.[81] but are not in agreement with the reported results[73,79,80] All the reported results of the enthalpy of mixing of Ag-Sn liquid solution measured by calorimetric measurements method[53,75,78,84,85] are in a reasonable agreement.

2.4 The Mg-Ag-Sn, Mg-Ag-Sn and Ag-In-Sn Systems

Kolesnichenko et al.[87] measured the isothermal section of the Mg-Ag-In system at 280 °C and the ternary isopleths with 50 In, 10 Ag and 30 Mg (wt.%) using XRD and metallographic methods.

Raynor and Frost[88] determined the isothermal sections in the Ag-rich area of the Mg-Ag-Sn system at 450 and 550 °C using optical microscopy and XRD. The isothermal section at 450 °C was also measured by Karonik et al.[89] by means of thermal analysis, optical microscopy, and XRD. The solubility of Sn in Mg_3Ag was found to be about 7 wt.%. Karonik et al.[89] also determined the ternary isoplethal sections at constant Sn of 10 and Ag of 10 wt.%.

Phase relations in the Ag-In-Sn system were studied by Korhonen and Kivilahti[90] with DSC, SEM, and optical microscopy, but no experimental data are tabulated or illustrated in their work. Liu et al.[91] reinvestigated phase equilibria in the system with DSC and metallography and determined the isothermal sections at 180, 250, 400, and 600 °C as well as ternary isoplethal sections with constant Ag of 10, 20, 30, and 40, and constant In of 20 and 40 (wt.%). Vassilev et al.[92] measured the isothermal section at 280 °C and a ternary isoplethal section at constant Ag of 2.5 (at.%) using DSC, XRD and SEM. Miki et al.[93] determined the activity of Ag in the liquid solution using Knudsen cell with mass spectrometry but none of his data are tabulated. Gather et al.[94] measured the enthalpy of mixing of the liquid phase by heat flow calorimetry with different molar ratios of Sn/In (1/4, 2/3, 3/2 and 4/1).

Table 2 Phase crystal structure and thermodynamic model used in present work

Phase	Pearson symbol	Strukturbericht designation	Space group	Prototype	Model
Liquid	...	...	...	...	MQMPA
fcc (Ag)	cF4	A1	$Fm\bar{3}m$	Cu	CEF
bct (In)	tI4	A5	$I4_1/mmm$	Sn	BW
bcc_A2 (MgAg)	cI2	A2	$Im\bar{3}m$	W	BW
hcp (Mg)	hP2	A3	$P6_3/mmc$	Mg	BW
tet (Sn)	tI2	A6	F4/mmm	In	BW
Mg_2Sn	cF12	C1	$Fm\bar{3}m$	CaF_2	ST
Ag_3Sn	oP8	D0a	Pmmm	Cu_3Ti	CEF
bcc_B2 (MgAg)	cP2	B2	$Pm\bar{3}m$	CsCl	CEF
Ag_3Mg	cP4	$L1_2$	$Pm\bar{3}m$	$AuCu_3$	CEF
$AgMg_3$	hP8	$D0_{18}$	$P6_3/mmc$	$AsNa_3$	CEF
$AgMg_4$	hP*	...	...	...	ST
$Ag_{17}Mg_{54}$	...	...	...	...	CEF
β'(MgIn)	cP4	$L1_2$	Pm3m	$AuCu_3$	CEF
β_1(MgIn)	hR16	...	R3m	...	CEF
β_2(MgIn)	hP9	...	$P\bar{6}2m$	Mg_2Tl	ST
β_3(MgIn)	oI28	$D8_g$	Ibam	Mg_5Ga_2	ST
β"(MgIn)	tP4	$L1_0$	P4/mmm	AuCu	CEF
γ'(MgIn)	cP4	$L1_2$	Pm3m	$AuCu_3$	CEF
β(InSn)	tI2	A6	F4/mmm	In	BW
γ(InSn)	hP5	...	P6/mmm	...	BW
Ag_2In	cP52	$D8_3$	$P\bar{4}3m$	Cu_9Al_4	CEF
Ag_3In	cP*	...	$Pm\bar{3}m$	...	ST
$AgIn_2$	tI12	C16	I4/mcm	Al_2Cu	ST

MQMPA: Modified Quasichemical Model in the Pair Approximation; CEF: Compound Energy Formalism; BW: Bragg-Willams model; ST: Stoichiometric compound

3. Thermodynamic Modeling

All the thermodynamic assessment status of sub-systems of Mg-Sn-Ag-In quaternary system are listed in Table 1. The Mg-Sn phase diagram was critically evaluated and optimized by Jung et al.[95,96] using the Modified Quasichemical Model in the Pair Approximation (MQMPA) for the liquid phase. Similarly, the In-Mg and In-Sn binary systems and the Mg-In-Sn ternary system were critically evaluated and optimized in our previous work[97] by using the MQMPA as well for the liquid phase. In order to construct a self-consistent thermodynamic database of Mg-base system, the thermodynamic parameters reported for the

Table 3 Equilibrium compositions of the Mg-Sn-Ag ternary system as determined in the present work

T (°C)	Alloy Nominal comp. (at. %)	Phase equilibria	Phase Compositions (at. %)								
			Phase 1			Phase 2			Phase 3		
		Phase 1/Phase 2/Phase 3	Mg	Sn	Ag	Mg	Sn	Ag	Mg	Sn	Ag
415	88Mg10Sn2Ag	hcp (Mg)/Mg_2Sn/Mg_3Ag	97.14	1.00	1.86	67.59	32.39	1.86	76.56	2.56	20.88
	80Mg10Sn10Ag	hcp (Mg)/Mg_2Sn/Mg_3Ag	96.85	1.02	2.13	67.55	32.43	2.13	75.34	2.31	22.35
	70Mg10Sn30Ag	bcc_B2/Mg_2 Sn/Mg_3 Ag	55.13	0.03	44.84	67.86	31.93	44.84	74.28	2.43	23.29
	50Mg20Sn30Ag	bcc_B2/Mg_2 Sn	35.83	11.44	52.73	67.32	32.41	52.73	···	···	···
	45Mg25Sn30Ag	bcc_B2/Mg_2 Sn/liquid	33.79	13.76	52.45	67.28	32.47	52.45	···	···	···
350	88Mg10Sn2Ag	hcp (Mg)/Mg_2Sn/Mg_3Ag	98.32	0.58	1.10	67.51	32.42	1.10	75.20	3.41	21.39
	80Mg10Sn10Ag	hcp (Mg)/Mg_2Sn/Mg_3Ag	98.34	0.57	1.09	67.86	32.10	1.09	76.02	2.18	21.80
	70Mg10Sn30Ag	bcc_B2/Mg_2 Sn/Mg_3 Ag	55.29	0.83	43.88	67.55	32.10	43.88	72.96	3.33	23.71
	50Mg20Sn30Ag	bcc_B2/Mg_2 Sn	35.85	11.21	52.94	67.54	32.20	52.94	···	···	···

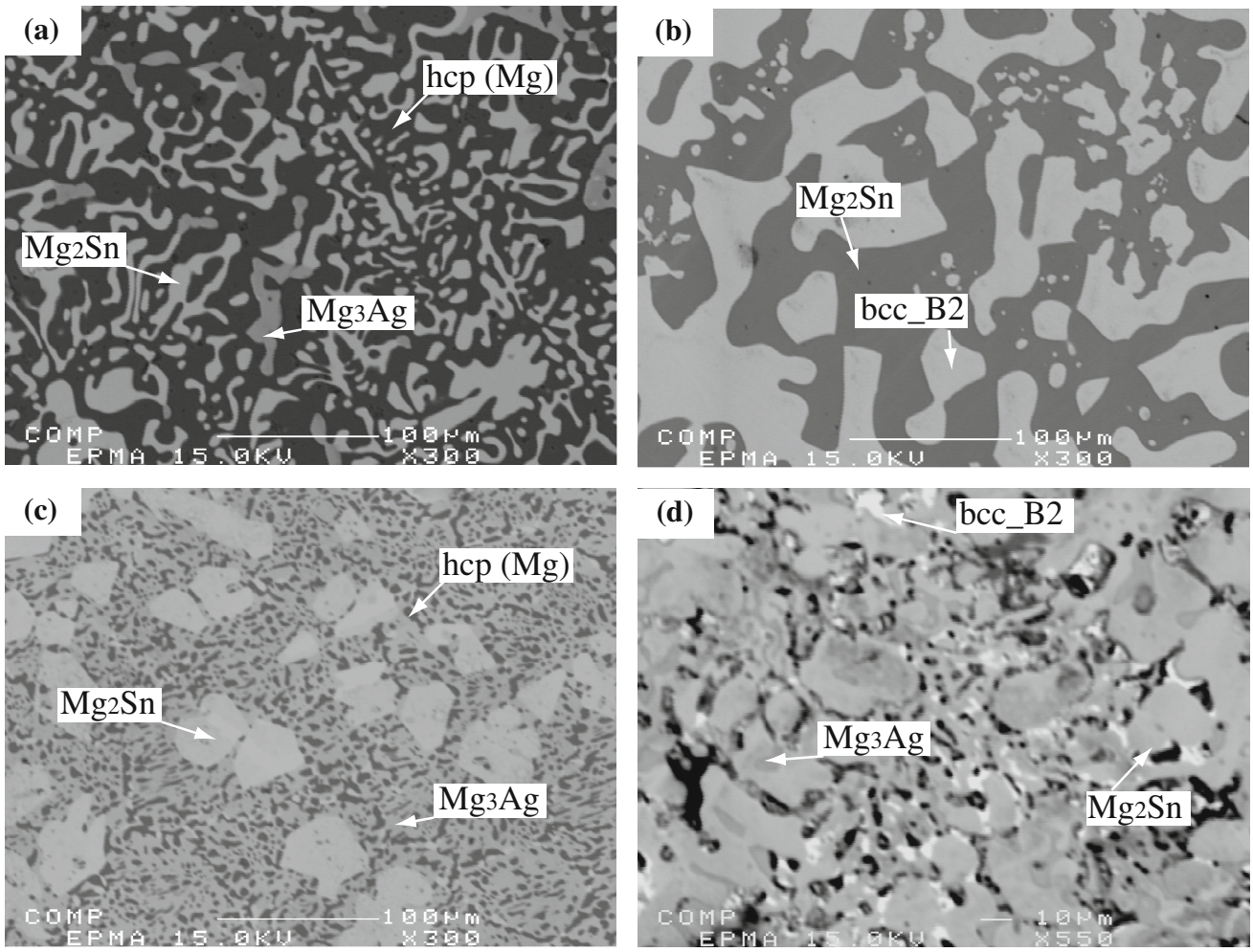

Fig. 1 BSE images of typical ternary alloys: (a) Mg88Sn10Ag2 alloy annealed at 415 °C for 25 days; (b) Mg50Sn20Ag30 alloy annealed at 415 °C for 25 days; (c) Mg80Sn10Ag10 alloy annealed at 350 °C for 40 days; (d) Mg60Sn10Ag30 (at. %) alloy annealed at 350 °C for 40 days

Mg-Sn,[95] In-Mg,[97] In-Sn,[97] and Mg-In-Sn[97] systems were thus used in the present work for the optimization of the whole Mg-Sn-Ag-In quaternary system.

The remaining binary systems, the Ag-Mg, Ag-In and Ag-Sn systems, were previously optimized by Lim et al.,[30] Moser et al.,[47] and Oh et al.,[98] respectively, using the

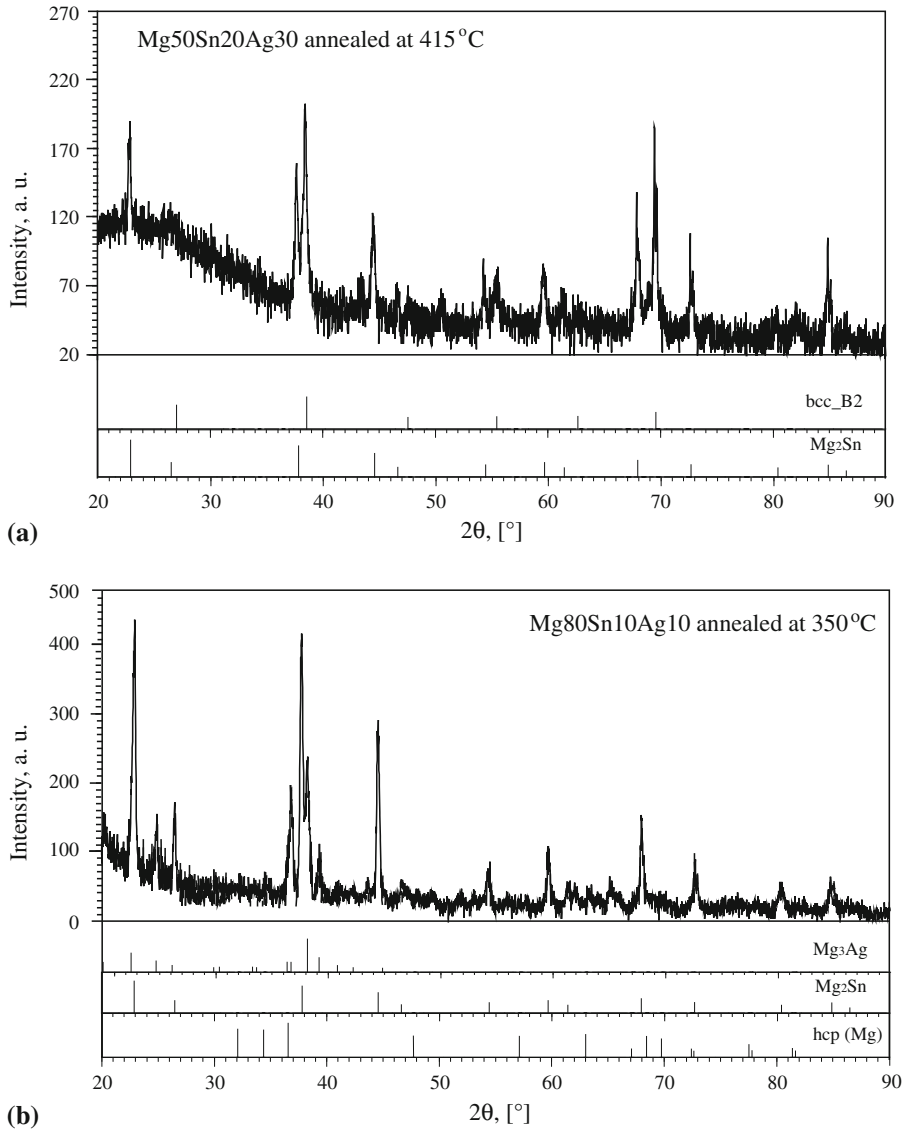

Fig. 2 XRD patterns of selected annealed samples: (a) Mg50Sn20Ag30 alloy annealed at 415 °C for 25 days, and (b) Mg80Sn10Ag10 alloy annealed at 350 °C for 40 days

Bragg-Williams Model (BWM)[100] for the liquid phase, which neglects short-range order. However, these assessments are inconsistent with some experimental data. For example, in the optimized work of the Ag-Mg system by Lim et al.,[30] Mg_3Ag and $Mg_{54}Ag_{17}$ are treated as a single stoichiometric compound, $Mg_{54}Ag_{17}$. In addition, although the bcc phase is modeled using two energy contribution parts, ordered bcc_B2 and disordered bcc_A2, the parameters of the ordered bcc_B2 part are given without considering the symmetry of the crystal structure. Another example is the Ag-In binary system optimized by Moser et al.[47]: the bcc and Ag_3In phases are missing. Moreover, no critical review of the experimental data is performed in the assessments of Lim et al.[30] and Moser et al.[47] Consequently, in the present work, all available phase diagram and thermodynamic data of the Ag-Mg, Ag-In and Ag-Sn binary systems were critically re-evaluated and optimized using the MQMPA for the liquid phase with the FactSage thermodynamic software.[101] All phases considered in the Mg-Sn-Ag-In quaternary system are summarized in Table 2 along with the model used to describe their thermodynamic properties.

3.1 Stoichiometric Phases

The molar Gibbs energies of pure elements and stoichiometric phases can be described by:

$$G_T^o = H_T^o - TS_T^o \quad \text{(Eq 1)}$$

$$H_T^o = \Delta H_{298K}^o + \int_{T=298.15K}^{T} C_p dT \quad \text{(Eq 2)}$$

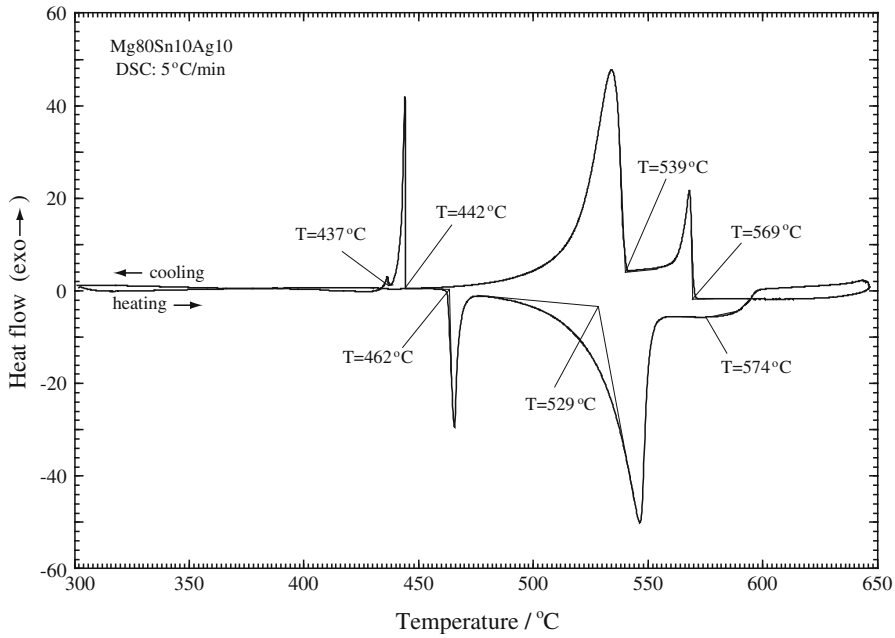

Fig. 3 The DSC curves of Mg80Sn10Ag10 alloy obtained in the present work

Table 4 Thermal signals obtained from DSC measurements of the Mg-Sn-Ag ternary system

	Thermal signal (°C)	
Sample (at.%)	**Heating**	**Cooling**
Mg88Sn10Ag2	568; 527; 462	569; 531; 444; 438
Mg80Sn10Ag10	574; 529; 462	569; 539; 442; 437
Mg60Sn10Ag30	678; 622	681; 625
Mg50Sn20Ag30	602; 562; 413	608; 573; 416
Mg45Sn25Ag30	528;415; 375; 199	533; 420; 191

$$S_T^o = S_{298K}^o + \int_{T=298.15K}^{T} (C_p/T)dT \qquad \text{(Eq 3)}$$

where $\Delta H^o_{298.15K}$ is the molar enthalpy of formation of a given species from pure elements (the $\Delta H^o_{298.15K}$ of any element stable at 298.15 K and 1 atm is assumed as 0 J/mol at the reference state), $S^o_{298.15K}$ is the molar entropy at 298.15 K, and C_p is the molar heat capacity.

In the present study, the Gibbs energy of pure elements were taken from the SGTE database.[100] As there are no experimental heat capacity data for Ag-In, Ag-Sn and Ag-Mg intermetallic phases, their heat capacities were evaluated using the Neumann-Kopp rule.[102] The heat capacity curves of solid In and Sn from the SGTE database show a maximum just above their melting points (that is in the liquid stable region). Several intermetallic phases in the studied system have their melting points substantially higher than the pure elements from which they are formed. The heat capacity functions of intermetallic phases obtained with the Neumann-Kopp rule had also such a maximum, which is little plausible. In order to resolve this problem, we modified the heat capacity functions of solid In and Sn above their melting points, that is extrapolated into the liquid region, to make sure that the heat capacity curves of intermetallic phases increase with temperature until their own melting points. This was solely applied when the Neumann-Kopp rule was employed for intermetallic phases and does not influence pure solid In and Sn which keep their SGTE Gibbs energy functions.

3.2 Solid Solutions

The Compound Energy Formalism (CEF) was introduced by Hillert[103] to describe the Gibbs energy of solid solutions. In this model, ideal mixing is assumed on each sub-lattice. In the present work, the Ag_3Mg, Ag_3Sn, $AgMg_3$, $Ag_{17}Mg_{54}$,β',β_1,β'',γ', and Ag_2In phases were modeled with the CEF. The stoichiometry of the sublattices was based on the crystal structures reported in the literature (Table 2). The Gibbs energy expression of the Ag_2In phase, for example, based on the CEF, is obtained by mixing In and Ag on two sublattices with a stoichiometric ratio of 2:1 as

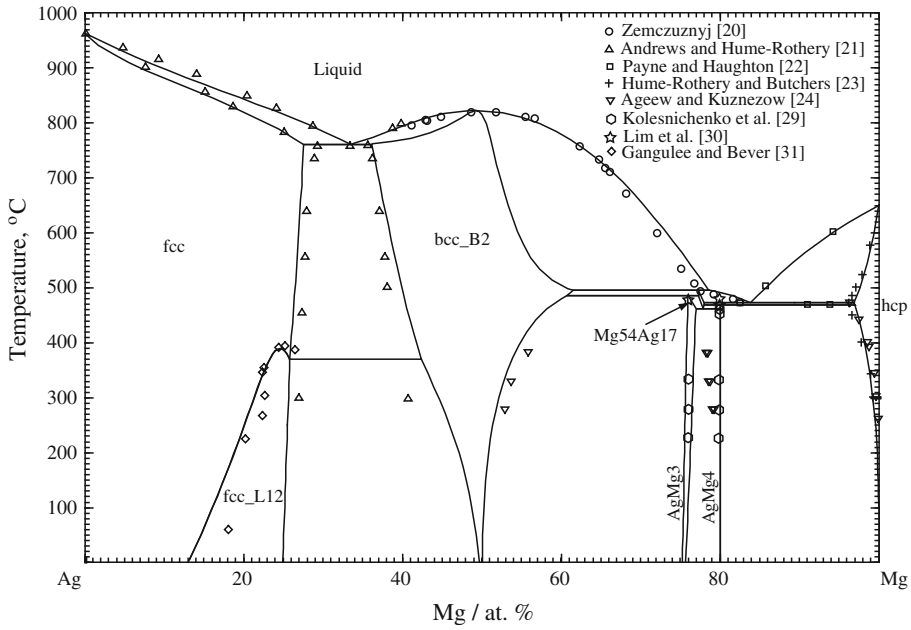

Fig. 4 Calculated phase diagram of Ag-Mg binary system compared with experimental data[20-24,29-31]

Table 5 Calculated invariant reactions in the Ag-Mg system compared with reported experimental values

Reaction	Reaction type	T (°C)	Composition (Mg at. %)			Reference
Liquid ↔ fcc + bcc_B2	Eutectic	759	33.4	29.3	35.5	[19]
		761	33.5	27.6	36.1	This work
Liquid ↔ bcc_B2	Congruent	820	50.0	50.0	···	[19]
		822	49.3	49.3	···	This work
Liquid + bcc_B2 ↔ $Mg_{54}Ag_{17}$	Peritectic	494	77.4	65.4	···	[19,29]
		494	78.6	61.4	77.2	This work
bcc_B2 + $Mg_{54}Ag_{17}$ ↔ $AgMg_3$	Peritectiod	484	···	···	···	[30]
		483	60.6	76.2	77.2	This work
Liquid ↔ $Mg_{54}Ag_{17}$ + hcp	Eutectic	472	82.4	···	96.2	[19,29]
		472	83.8	78.0	97.0	This work
$Mg_{54}Ag_{17}$ + hcp ↔ $AgMg_4$	Peritectoid	465	···	···	···	[29]
		469	77.0	96.0	80.0	[30]
		467	78.0	96.9	80.0	This work
$Mg_{54}Ag_{17}$ ↔ $AgMg_4$ + $AgMg_3$	Eutectoid	464	77.5	80.0	77.9	This work
fcc ↔ fcc_L12 + bcc_B2	Eutectoid	370	25.8	25.8	42.3	This work
fcc ↔ Ag_3Mg	Congruent	392	···	···	···	[19]
		390	24.4	24.4	···	This work

$(Ag)_2$ (Ag, In). The Gibbs energy of the Ag_2In solution is then expressed as:

$$G^{Ag_2In} = y^{I}_{Ag}y^{II}_{In}G^{o}_{Ag:In} + y^{I}_{Ag}y^{II}_{Ag}G^{o}_{Ag:Ag} + RT(y^{II}_{Ag}\ln y^{II}_{Ag} + y^{II}_{In}\ln y^{II}_{In}) + y^{I}_{Ag}y^{II}_{Ag}y^{II}_{In}{}^{n}L_{Ag:Ag,In} \quad \text{(Eq 4)}$$

where y^{II}_{Ag} and y^{II}_{In} are the site fractions of Ag and In on the second sublattice. $G^{o}_{Ag:In}$ and $G^{o}_{Ag:Ag}$ are the Gibbs energy of Ag_2In and Ag_2Ag, respectively. ${}^{n}L_{Ag:Ag,In}$ is the interaction energy between Ag and In on the second sublattice. Similarly, the Gibbs energy functions of all other solid solutions are described according to the structure of their sublattice using the CEF.

The sublattice model, developed by Hillert,[103] allows the description of a variety of solid solutions with mathematical functions, particularly for the ordered phase. The sublattice formalism applied to the A2 and B2 phases was introduced by Dupin and Ansara[104] and the same notations were used in the present work. The Gibbs energy functions of the bcc_A2 and bcc_B2 phases were model as single bcc phases with sublattice structures as disordered (Ag, In, Mg, Sn)$(Va)_3$ and ordered (Ag, In, Mg, Sn)(Ag, In, Mg, Sn)$(Va)_3$ parts. The molar Gibbs energy of these disordered and ordered parts can be expressed as:

$$G^{bcc} = {}^{dis}G^{bcc\_A2} + {}^{ord}G^{bcc\_B2} \quad \text{(Eq 5)}$$

where ${}^{dis}G^{bcc\_A2}$ is the Gibbs energy contribution of the bcc phase from the disordered part (bcc_A2), which can be expressed as follows:

$$\begin{aligned} {}^{dis}G^{bcc\_A2} = & \sum_{i=Ag,In,Mg,Sn} x_i {}^{o}G_i^{bcc\_A2} + RT(x_{Ag}\ln x_{Ag} \\ & + x_{In}\ln x_{In} + x_{Mg}\ln x_{Mg} + x_{Sn}\ln x_{Sn}) \\ & + x_i x_j \sum_{n=0}^{n} (x_i - x_j)^n {}^nL_{i,j}^{dis} + x_i x_j x_k \sum_{m=0,1,and2} {}^mL_{i,j,k}^{dis} \end{aligned} \quad \text{(Eq 6)}$$

In this expression, ${}^nL_{i,j}^{dis}$ and ${}^mL_{i,j,k}^{dis}$ are the binary and ternary interaction parameters of the disordered part of the bcc phase (bcc_A2).

In Eq 5, ${}^{ord}G^{bcc\_B2}$ is the Gibbs energy contribution of the bcc phase from the ordered part (bcc_B2), which can be expressed as follows:

$$\begin{aligned} {}^{ord}G^{bcc\_B2} = & \sum_{i\neq j} y_i^I y_j^{Iio} G_{i:j}^{bcc\_B2} \\ & + RT(y_i^I \ln y_i^I + y_j^I \ln y_j^I + \cdots) + RT(y_i^{II} \ln y_i^{II} \\ & + y_j^{II} \ln y_j^{II} + \cdots) + \Delta^{ord}G^{bcc\_B2} \end{aligned} \quad \text{(Eq 7)}$$

where $G_{i:j}^{bcc\_B2}$ is the Gibbs energy of the hypothetical compound ij, and $\Delta^{ord}G^{bcc\_B2}$ is the excess Gibbs energy of ordered part (bcc_B2), which is constituted of the binary and ternary interaction parameters $\Delta^{ord}G_{binary}^{bcc\_B2}$ and $\Delta^{ord}G_{ternary}^{bcc\_B2}$, which are expressed as:

$$\Delta^{ord}G_{binary}^{bcc\_B2} = y_i^I y_j^I \sum_{n=0}^{n} (y_i^I - y_j^I)^n {}^nL_{i,j:i}^I + y_i^{II} y_j^{II} \sum_{n=0}^{n} (y_i^{II} - y_j^{II})^n {}^nL_{i:i,j}^{II} \quad \text{(Eq 8)}$$

$$\begin{aligned} \Delta^{ord}G_{ternary}^{bcc\_B2} = & y_i^I y_j^I \sum_{n=0}^{n} (y_i^{II} - y_j^{II})^n {}^nP_{i,j:k}^I \\ & + y_i^{II} y_j^{II} \sum_{n=0}^{n} (y_i^{II} - y_j^{II})^n {}^nP_{k:i,j i\neq j\neq k}^{II} + (y_i^I y_j^I y_k^I {}^nP_{i,j,k:l}^I \\ & + y_i^{II} y_j^{II} y_k^{II} {}^nP_{l:i,j,k}^{II})_{l=i,j,or and i\neq j\neq k} \end{aligned} \quad \text{(Eq 9)}$$

where ${}^nL_{i,j:i}^I$ and ${}^nL_{i:i,j}^{II}$ are the binary interaction parameters of the ordered part bcc_B2, and ${}^nP_{i,j:k}^I$, ${}^nP_{k:i,j}^{II}$, ${}^nP_{i,j,k:l}^I$, and ${}^nP_{l:i,j,k}^{II}$ are the ternary interaction parameters of the ordered part bcc_B2. Due to the crystallographic symmetry of the bcc_B2 phase, the following relations are introduced:

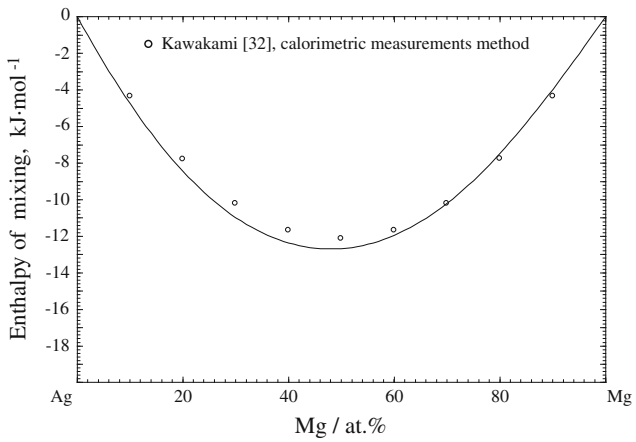

Fig. 5 Calculated enthalpy mixing of liquid phase of Ag-Mg system at 1050 °C compared with experimental data[32]

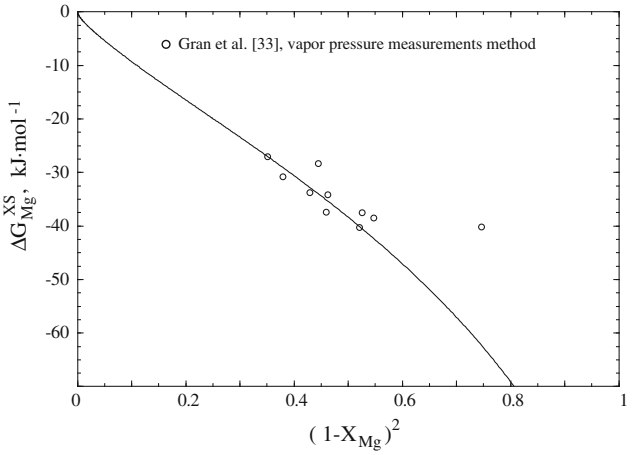

Fig. 6 Calculated ΔG_{Mg}^{xs} versus $(1\text{-}x_{Mg})^2$ of liquid phase at the temperature of 1400 °C along with the experimental data[33]

Table 6 Optimized model binary parameters of the MQM for liquid Mg-Sn-Ag-In alloys

Coordination numbers(a)					
i	**j**	Z_{ij}^i	Z_{ij}^j	**Gibbs energies of pair exchange reactions (J/mol)**	**Reference**
Mg	In	3	6	$g_{MgIn} = -9790.6 - 2092X_{InIn} - 209.2X_{InIn}^2$	[97]
Mg	Sn	4	8	$g_{MgSn} = -15263.2 - 0.88 \times T + (3347.2 + 0.42 \times T)X_{MgMg}$	[95]
Mg	Ag	7	7	$\Delta g_{MgAg} = -11129.4 + 0.08\times T + (-3933.0 + 0.13\times T)X_{AgAg} - 2594.1X_{MgMg}$	This work
Ag	In	3	7	$\Delta g_{AgIn} = -7112.8 - 1.26\times T + 1255.2X_{AgAg} + (2825.8 - 0.84\times T)X_{InIn}$	This work
Ag	Sn	3	7	$\Delta g_{AgSn} = -3723.8 - 2.30\times T + (-3347.2 + 1.26\times T)X_{AgAg} + (6276 - 3.35\times T)X_{SnSn}$	This work
Sn	In	6	6	$\Delta g_{SnIn} = -175.7 - 138.1X_{SnSn} - 133.9X_{InIn}$	[97]

(a) For all pure elements (Mg, Ag, In and Sn), $Z_{ii}^i = 6$

Table 7 Optimized model parameters for phases in the quaternary Mg-Sn-Ag-In system

Phase, model and thermodynamic parameters (J/mol or J/mol K)	Reference
Liquid phase	
$q^{001}_{InSn(Mg)} = -9204.8$,	This work
$q^{001}_{AgIn(Mg)} = q^{001}_{AgMg(In)} = q^{001}_{MgIn(Ag)} = 251.0 - 7.32\times T$	This work
$q^{001}_{AgIn(Sn)} = 2301.2 - 2.93\times T$, $q^{001}_{AgSn(In)} = 2301.2 - 0.42\times T$, $q^{001}_{InSn(Ag)} = 2301.2 - 2.51\times T$	This work
$q^{001}_{AgMg(Sn)} = -5020.8$, $q^{001}_{AgSn(Mg)} = -12552.0$	This work
hcp_A3(Mg) phase, (Ag, In, Mg, Sn):	
$G_{Mg} = {}^{0}G_{Mg}^{hcp}$, $G_{Ag} = {}^{0}G_{Ag}^{fcc} + 300 - 0.3\times T$	
$G_{Sn} = {}^{*}G_{Sn} + 3900 - 4.4\times T$, $G_{In} = {}^{*}G_{In} + 533 - 0.69\times T$,	This work
${}^{1}L_{Mg,Sn} = 48116$,	[95]
${}^{0}L_{Mg,In} = -28451 + 6.09\times T$, ${}^{1}L_{Mg,In} = -10460 + 5.44\times T$	[97]
${}^{0}L_{Ag,Sn} = -6024.9 + 10.96\times T$, ${}^{1}L_{Ag,Sn} = 43095.2 - 3.56\times T$	This work
${}^{0}L_{Ag,In} = -15815.5 + 15.23\times T$, ${}^{1}L_{Ag,In} = 74140.5 - 11.84\times T$, ${}^{2}L_{Ag,In} = 46233.2 - 6.28\times T$	This work
${}^{0}L_{Ag,Mg} = -33472.0 - 2.09\times T$, ${}^{1}L_{Ag,Mg} = 15899.2$	This work
${}^{0}L_{Ag,Mg,Sn} = -142256.0 + 8.37\times T$, ${}^{1}L_{Ag,Mg,Sn} = -148532.0 + 8.37\times T$, ${}^{2}L_{Ag,Mg,Sn} = 41840.0$	This work
${}^{0}L_{Ag,Mg,In} = {}^{1}L_{Ag,Mg,In} = {}^{2}L_{Ag,Mg,In} = 29288.0$	This work
${}^{0}L_{Ag,In,Sn} = {}^{1}L_{Ag,In,Sn} = {}^{2}L_{Ag,In,Sn} = 71128.0 - 4.18\times T$	This work
fcc_A1 phase, (Ag, In, Mg, Sn):	
$G_{Mg} = {}^{0}G_{Mg}^{hcp} + 2600 + 0.90\times T$, $G_{Ag} = {}^{0}G_{Ag}^{fcc}$	
$G_{In} = {}^{*}G_{In} + 123 - 0.30\times T$, $G_{Sn} = {}^{*}G_{Sn} + 4150 - 5.2\times T$	This work
${}^{0}L_{In,Sn} = 8368.0$; ${}^{0}L_{Ag,Sn} = -3138.0 + 10.04\times T$, ${}^{1}L_{Ag,Sn} = 42258.4 - 7.53\times T$	This work
${}^{0}L_{In,Mg} = -29915.6 - 1.88\times T$, ${}^{1}L_{In,Mg} = -13723.5 - 1.46\times T$, ${}^{2}L_{In,Mg} = -6276.0$	[97]
${}^{0}L_{Ag,In} = -18828.0 + 13.22\times T$, ${}^{1}L_{In,Ag} = 36819.2 - 9.29\times T$	This work
${}^{0}L_{Ag,Mg} = -52592.9 + 9.04\times T$, ${}^{1}L_{Ag,Mg} = 29288.0 - 10.88\times T$, ${}^{2}L_{Ag,Mg} = 3347.2 + 3.35\times T$	This work
${}^{0}L_{Ag,Mg,Sn} = -20920 - 16.74\times T$; ${}^{1}L_{Ag,Mg,Sn} = -8368 - 8.37\times T$; ${}^{0}L_{Ag,Mg,Sn} = -54392.0 - 16.74\times T$	This work
${}^{0}L_{Ag,In,Mg} = {}^{1}L_{Ag,In,Mg} = {}^{2}L_{Ag,In,Mg} = 41840.0$	
${}^{0}L_{Ag,In,Sn} = {}^{1}L_{Ag,In,Sn} = {}^{2}L_{Ag,In,Sn} = 43932.0 + 4.18\times T$	This work
bct(Sn) phase, (Ag, In, Mg, Sn):	
$G_{Mg} = {}^{0}G_{Mg}^{hcp} + 15000$, $G_{Ag} = {}^{0}G_{Ag}^{fcc} + 4184$,	This work
$G_{In:Va} = {}^{*}G_{In} + 2092$, $G_{Sn:Va} = {}^{*}G_{Sn}$	This work
${}^{0}L_{In,Sn:Va} = 460.2$, ${}^{0}L_{Ag,Sn:Va} = 18828.0$	This work
tet(In) phase, (Ag, In, Mg, Sn):	
$G_{In} = {}^{*}G_{In}$, $G_{Sn} = {}^{*}G_{Sn} + 15000$, $G_{Mg} = {}^{0}G_{Mg}^{hcp} + 15000$, $G_{Ag} = {}^{0}G_{Ag}^{hcp} + 15000$	This work
${}^{0}L_{In,Sn} = 836.8 - 1.67\times T$, ${}^{0}L_{In,Mg} = -26359.2 + 18.83\times T$	This work
β″ phase, (Mg, In)(Mg, In):	
$G_{Mg:Mg} = {}^{0}G_{Mg}^{hcp} + 2600 + 0.90\times T$, $G_{In:In} = {}^{*}G_{In} + 123 - 0.30\times T$,	[97]
$G_{Mg:In} = G_{In:Mg} = {}^{*}G_{In} + {}^{0}G_{Mg}^{hcp} - 9204.8 - 0.60\times T$,	[97]
${}^{0}L_{Mg,In:Mg} = {}^{0}L_{Mg:Mg,In} = -21756 - 0.63\times T$, ${}^{0}L_{Mg,In:In} = {}^{0}L_{In:Mg,In} = 418.4 - 0.42\times T$,	[97]
β′, γ′ phase, $(Ag, Mg, In)_3(Ag, Mg, In)$:	
$G_{Mg:Mg} = 4\times{}^{0}G_{Mg}^{hcp} + 10400 + 3.6\times T$, $G_{In:In} = 4\times{}^{*}G_{In} + 492 - 1.20\times T$,	[97]
$G_{Mg:In} = {}^{*}G_{In} + 3\times{}^{0}G_{Mg}^{hcp} + 7923.0\times + 2.4T$, $G_{In:Mg} = 3\times{}^{*}G_{In} + {}^{0}G_{Mg}^{hcp} - 35540.5 - 1.09\times T$	[97]
${}^{0}L_{In:Mg,In} = -32049.4 + 2.93\times T$, ${}^{1}L_{In:Mg,In} = 7949.6$,	[97]
$G_{Ag:Ag} = {}^{0}G_{Ag}^{fcc}$, $G_{Mg:Ag} = {}^{0}G_{Ag}^{fcc} + 3\times{}^{0}G_{Mg}^{hcp} + 1751.0$; $G_{Ag:Mg} = {}^{0}G_{Mg}^{hcp} + 3\times{}^{0}G_{Ag}^{fcc} - 53568 - 0.84\times T$	This work
Ag_2In phase, (Ag, In, Sn)$(Ag)_2$:	
$G_{In:Ag} = 2\times{}^{0}G_{Ag}^{fcc} + {}^{*}G_{In} - 21764.0 + 21.3\times T$, $G_{Ag:Ag} = 3\times{}^{0}G_{Ag}^{fcc}$, $G_{Sn:Ag} = 2\times{}^{0}G_{Ag}^{fcc} + {}^{*}G_{Sn} - 4184.0$	This work
${}^{0}L_{Ag,In:Ag} = -4184.0$, ${}^{0}L_{Ag,Sn:Ag} = -3347.2 - 3.35\times T$	This work
$AgMg_3$ phase, (Ag, In, Mg, Sn)(In, Mg, $Sn)_3$:	
$G_{Ag:Mg} = {}^{0}G_{Ag}^{fcc} + 3\times{}^{0}G_{Mg}^{hcp} - 41492.7 + 1.17\times T$, $G_{Mg:Mg} = 4\times{}^{0}G_{Mg}^{hcp} + 16317.6$;	This work
$G_{Ag:In} = {}^{0}G_{Ag}^{fcc} + 3\times{}^{*}G_{In} + 20920.0$, $G_{Mg:In} = {}^{0}G_{Mg}^{hcp} + 3\times{}^{*}G_{In} + 418.5$, $G_{In:In} = 4\times{}^{*}G_{In} + 418.5$	This work
$G_{In:Mg} = 3\times{}^{0}G_{Ag}^{fcc} + {}^{*}G_{In} + 418.5$, $G_{Sn:Mg} = 3\times{}^{0}G_{Mg}^{hcp} + {}^{*}G_{Sn}$, $G_{Mg:Sn} = {}^{0}G_{Mg}^{hcp} + 3\times{}^{*}G_{Sn} + 4184.5$	This work
$G_{In:Sn} = {}^{*}G_{Sn} + 3\times{}^{*}G_{In} + 4184.8$, $G_{Sn:In} = 3\times{}^{*}G_{Sn} + {}^{*}G_{In} + 4184.5$	This work
$G_{Ag:Sn} = {}^{0}G_{Ag}^{fcc} + 3\times{}^{*}G_{Sn} + 4184.8$, $G_{Sn:Sn} = 4\times{}^{*}G_{Sn} + 4184.5$	This work
${}^{0}L_{Ag,Mg:Mg} = -17865.7 + 20.92$, ${}^{0}L_{Ag:In,Mg} = -119244$, ${}^{0}L_{Ag,In:Mg} = -35564$	This work
${}^{0}L_{Ag,Sn:Mg} = {}^{0}L_{Ag,Mg:Sn} = {}^{0}L_{Ag:Mg,Sn} = -112968.0 + 54.39\times T$	This work
$Ag_{17}Mg_{54}$ phase, (Ag, Mg, $Sn)_{17}(Mg)_{54}$:	
$G_{Ag:Mg} = 17\times{}^{0}G_{Ag}^{fcc} + 54\times{}^{0}G_{Mg}^{hcp} - 569664.2 - 161.08\times T$; $G_{Mg:Mg} = 71\times{}^{0}G_{Mg}^{hcp} + 891192$;	This work

Table 7 continued

Phase, model and thermodynamic parameters (J/mol or J/mol K)	Reference
$G_{Sn:Mg} = 17\times{}^{*}G_{Sn} + 54\times{}^{0}G_{Mg}^{hcp}$	This work
${}^{0}L_{Ag,Mg:Mg} = -912112 + 209.2\times T$, ${}^{0}L_{Ag,Sn:Mg} = -1317960.0 + 33.47\times T$	This work
β_1(hR16) phase, (Mg, In)$_3$(Mg, In):	
$G_{Mg:Mg} = 4\times{}^{0}G_{Mg}^{hcp} + 6694.4$, $G_{In:In} = 4\times{}^{*}G_{In}$,	This work
$G_{Mg:In} = {}^{*}G_{In} + 3\times{}^{0}G_{Mg}^{hcp} - 35145.6 + 3.18\times T$, $G_{In:Mg} = 3\times{}^{*}G_{In} + {}^{0}G_{Mg}^{hcp}$	This work
γ(InSn) phase, (In, Sn):	
$G_{In} = {}^{*}G_{In} + 10292.6 - 7.64\times T$, $G_{Sn} = {}^{*}G_{Sn} + 924.7 - 1.76\times T$,	[97]
${}^{0}L_{In,Sn} = -15480.8 + 18.74\times T$	
β(InSn) phase, (In, Sn):	
$G_{In:Va} = {}^{*}G_{In}$, $G_{Sn:Va} = {}^{*}G_{Sn} + 5015.5 - 7.50\times T$,	[97]
${}^{0}L_{In,Sn:Va} = 292 - 3.14\times T$, ${}^{1}L_{In,Sn:Va} = 627.6 + 0.29\times T$	
Mg_2Snphase, $(Mg)_2(Sn)$:	
$G = -102589.8 + 367.5\times T - 68.331\times T \ln T - 0.0178986\times T^2 + 3.33829\times 10^{-7}\times T^3 + 95940/T$	[95]
bcc_B2 phase, (Ag, In, Mg, Sn)(Ag, In, Mg, Sn)	
$G_{Mg:Ag} = G_{Ag:Mg} = -22593.6 + 3.82\times T$, $G_{In:Ag} = G_{Ag:In} = 8267.6 + 1.36\times T$	This work
$G_{Mg:In} = G_{In:Mg} = -2092 + 2.09\times T$	This work
${}^{0}L_{Ag,Mg:Ag} = {}^{0}L_{Ag:Ag,Mg} = 37237.6 - 0.05\times T$, ${}^{0}L_{Ag,Mg:Mg} = {}^{0}L_{Mg:Ag,Mg} = 8368 - 0.05\times T$	This work
${}^{1}L_{Ag,Mg:Ag} = {}^{1}L_{Ag,Mg:Mg} = {}^{1}L_{Mg:Ag,Mg} = {}^{1}L_{Ag:Ag,Mg} = -4811.6 + 1.26\times T$	This work
${}^{0}L_{Ag,In:Ag} = {}^{0}L_{Ag:Ag,In} = 28350.8 + 1.36\times T$, ${}^{0}L_{Ag,In:In} = {}^{0}L_{In:Ag,In} = -11815.6 + 1.36\times T$	This work
${}^{1}L_{Ag,In:Ag} = {}^{1}L_{Ag,In:In} = {}^{1}L_{In:Ag,In} = {}^{1}L_{Ag:Ag,In} = -6694.4$	This work
${}^{0}L_{Ag,Mg:In} = {}^{0}L_{In:Ag,Mg} = -33472 - 0.84\times T$	This work
${}^{0}L_{Ag,Mg:Sn} = {}^{0}L_{Sn:Ag,Mg} = -48952.8$, ${}^{0}L_{Mg,Sn:Ag} = {}^{0}L_{Ag:Mg,Sn} = -50626.4$	This work
$AgMg_4$phase, $(Ag)(In, Mg)_4$	This work
$G_{Ag:Mg} = 4\times G_{Mg}^{hcp} + G_{Ag}^{fcc} - 55980 + 19.07\times T$, $G_{Ag:In} = 4\times{}^{*}G_{In} + G_{Ag}^{fcc}$	
Ag_3Snphase, (Ag, Mg, Sn)$_3$(Sn)	This work
$G_{Ag:Sn} = 3\times G_{Ag}^{fcc} + {}^{*}G_{Sn} - 18430.5 - 8.91\times T$, $G_{Mg:Sn} = 3\times G_{Mg}^{hcp} + {}^{*}G_{Sn}$	This work
$G_{Sn:Sn} = 4\times{}^{*}G_{Sn} + 58576.0$	
$AgIn_2$phase, $(Ag)(In)_2$:$G = G_{Ag}^{fcc} + 2\times{}^{*}G_{In} - 21764 + 21.3\times T$	This work
Ag_3Inphase, $(Ag)_3(Ag, In)$	
$G_{Ag:In} = 3\times G_{Ag}^{fcc} + {}^{*}G_{In} - 30982.5$, $G_{Ag:Ag} = 4\times G_{Ag}^{fcc}$, ${}^{0}L_{Ag:Ag,In} = -12296.8 + 71.55\times T$	This work
Ag_2Inphase, $(Ag)_2(Ag, In, Sn)$	
$G_{Ag:In} = 2\times G_{Ag}^{fcc} + {}^{*}G_{In} - 23790.2 - 1.33\times T$, $G_{Ag:Ag} = 3\times G_{Ag}^{fcc}$, $G_{Ag:Sn} = 2\times G_{Ag}^{fcc} + {}^{*}G_{Sn} - 4184.0$	This work
${}^{0}L_{Ag:Ag,In} = -4184.0$, ${}^{0}L_{Ag:Ag,Sn} = -5439.2 - 7.95\times T$	This work
bcc_B2 phase, (Ag, In, Mg, Sn)(Ag, In, Mg, Sn)	
$G_{Mg:Ag} = G_{Ag:Mg} = -22593.6 + 3.82\times T$, $G_{In:Ag} = G_{Ag:In} = 8267.6 + 1.36\times T$	This work
$G_{Mg:In} = G_{In:Mg} = -2092 + 2.09\times T$	This work
${}^{0}L_{Ag,Mg:Ag} = {}^{0}L_{Ag:Ag,Mg} = 37237.6 - 0.05\times T$, ${}^{0}L_{Ag,Mg:Mg} = {}^{0}L_{Mg:Ag,Mg} = 8368 - 0.05\times T$	This work
${}^{1}L_{Ag,Mg:Ag} = {}^{1}L_{Ag,Mg:Mg} = {}^{1}L_{Mg:Ag,Mg} = {}^{1}L_{Ag:Ag,Mg} = -4811.6 + 1.26\times T$	This work
${}^{0}L_{Ag,In:Ag} = {}^{0}L_{Ag:Ag,In} = 28350.8 + 1.36\times T$, ${}^{0}L_{Ag,In:In} = {}^{0}L_{In:Ag,In} = -11815.6 + 1.36\times T$	This work
${}^{1}L_{Ag,In:Ag} = {}^{1}L_{Ag,In:In} = {}^{1}L_{In:Ag,In} = {}^{1}L_{Ag:Ag,In} = -6694.4$	This work
$InMg_2$phase, $(In)(Mg)_2$:$G = 2\times G_{Mg}^{hcp} + {}^{*}G_{In} - 29022.64 + 1.09\times T$	This work
In_2Mg_5phase, $(In)_2(Mg)_5$:$G = 5\times G_{Mg}^{hcp} + 2\times{}^{*}G_{In} - 65022.3 + 5.14\times T$	This work
fcc_L12 phase, (Ag, Mg)(Ag, Mg)$_3$	
$G_{Mg:Ag} = 4184.0$, $G_{Ag:Mg} = -2092$	This work
${}^{0}L_{Ag:Ag,Mg} = -3430.9 + 27.87\times T$, ${}^{0}L_{Mg:Ag,Mg} = 12259.1 + 36.23\times T$, ${}^{0}L_{Ag,Mg:Ag} = 2343.0 + 12.64\times T$	This work
${}^{0}L_{Ag,Mg:Mg} = -795.0 + 10.96\times T$, ${}^{1}L_{Ag:Ag,Mg} = {}^{1}L_{Mg:Ag,Mg} = 43095.2 + 33.89\times T$	This work

$${}^{*}G_{In} = \int {}^{*}Cp_{In}dt - T\times\int\frac{{}^{*}Cp_{In}}{T}dt, \quad {}^{*}G_{Sn} = \int {}^{*}Cp_{Sn}dt - T\times\int\frac{{}^{*}Cp_{Sn}}{T}dt$$

$$\begin{aligned} *Cp_{Sn} &= 25.858 - 0.0010237\times T - 36880/T^{-2} + 1.9156602\times 10^{-5}\times T^2 \quad 249\ K < T < 250K \\ &= 15.961 + 0.0377404\times T + 123920/T^{-2} - 1.8727002\times 10^{-5}\times T^2 \quad 251\ K < T < 1000\ K \\ &= 35.098\,506\ K < T < 3000\ K \end{aligned}$$

$$\begin{aligned} {}^{*}C_p(In) &= 21.8386 + 0.01145132\times T + 45812\times T^{-2} + 1.2721926\times 10^{-5}\times T^2 \quad 298\ K < T < 429.78\ K \\ &= 31.05 - 0.0001919\times T - 312000\times T^{-2} + 3.374\times 10^{-8}\times T^2 \quad 429.79\ K < T < 3800\ K \end{aligned}$$

Table 8 Calculated invariant reactions in the Ag-In system compared with experimental data

Reaction	Reaction type	Temperature (°C)	Composition (In at.%)			Reference
hcp + fcc ↔ Ag_3In	Peritectiod	187	20.0	···	···	[46]
		187	21.8	18.0	21.6	This work
Liquid + fcc ↔ bcc	Peritectic	695	29.5	21	25.0	[46]
		697	29.4	18.6	24.0	This work
fcc + bcc ↔ hcp	Peritectiod	670	20.9	···	25.0	[46]
		667	20.2	25.3	23.6	This work
bcc ↔ liquid + hcp	Remelting	660	29.0	32.5	···	[46]
		660	26.7	33.4	24.6	This work
hcp ↔ liquid + Ag_2In	Remelting	205	45.9	92.2	33.5	[46]
		205	36.1	93.1	33.3	This work
Liquid + Ag_2In ↔ $AgIn_2$	Peritectic	166	···	33.5	···	[46]
		163	95.8	33.3	66.7	This work
Liquid ↔ $AgIn_2$ + tet(In)	Eutectic	144	96.8	···	···	[46]
		144	97.2	66.7	100	This work
hcp ↔ Ag_2In	Congruent	312	···	···	···	[46]
		313	33.3	33.3	···	This work

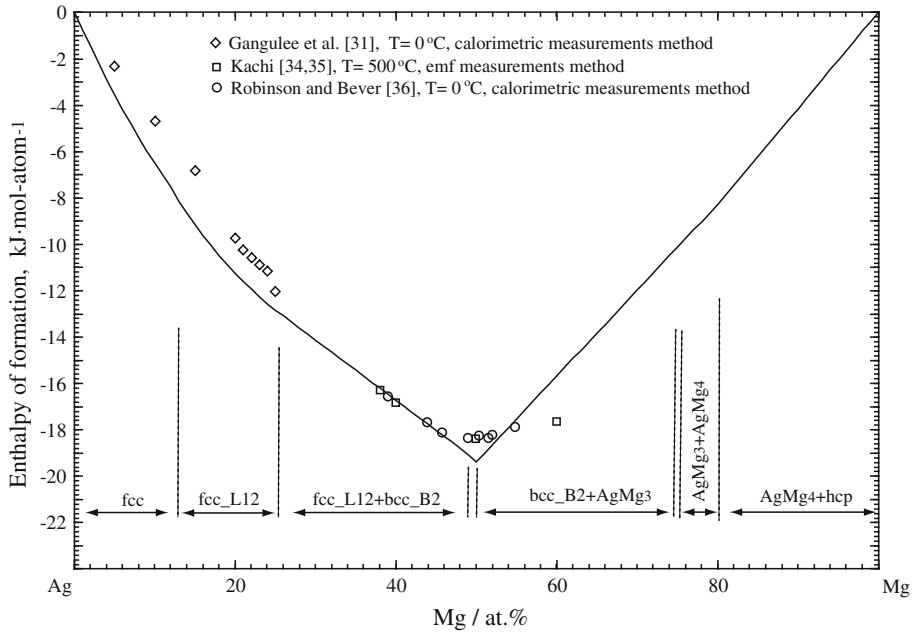

Fig. 7 Calculated heat formation of solid phases at 25 °C compared with experimental data[31,34-36]

$$ {}^{o}G_{i:j}^{bcc\_B2} = {}^{o}G_{j:i}^{bcc\_B2};\ {}^{n}L_{i,j:i}^{I} = {}^{n}L_{i:i,j}^{II};\ {}^{n}P_{i,j:k}^{I} = {}^{n}P_{k:i,j}^{II},\ {}^{n}P_{i,j,k:l}^{I} = {}^{n}P_{l:i,j,k}^{II} \quad \text{(Eq 10)} $$

Also, relations exist for the parameters between the ordered and disordered solutions which are used in the present work and are described in details in the reference.[104]

The disorder solid solutions hcp (Mg-rich), bct (Sn-rich), tetatrahedral (In-rich), bcc, β(InSn), and γ(InSn) were modeled with one sublattice as (Ag, Mg, Sn), a subregular solution approximation is used for the excess Gibbs energy and the configurational entropy if of Bragg-Williams type.

3.3 Liquid Phase

The thermodynamic properties of the liquid phase were modeled using the Modified Quasichemical Model in the Pair Approximation (MQMPA) developed by Pelton

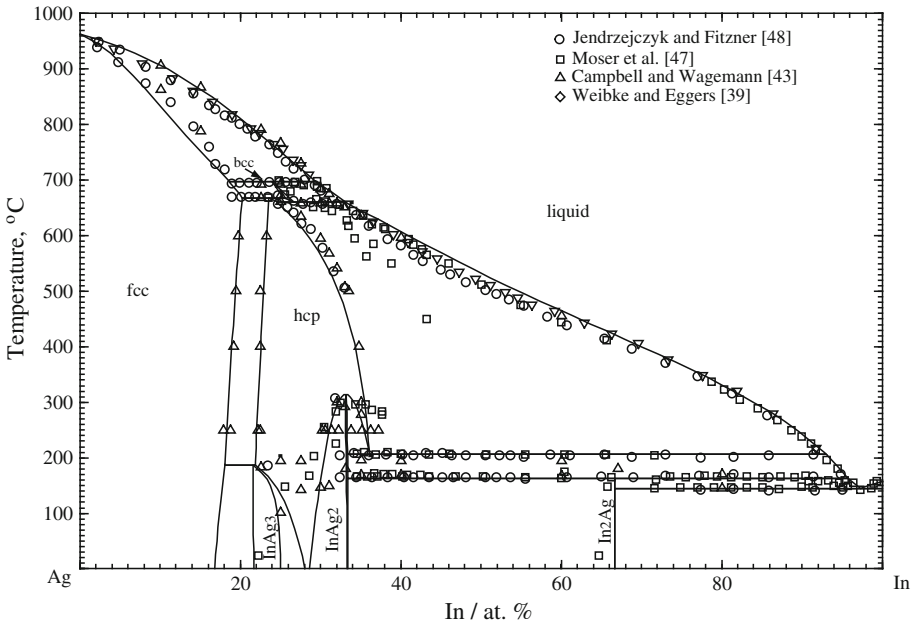

Fig. 8 Calculated phase diagram of Ag-In system compared with experimental data[39,43,47,48]

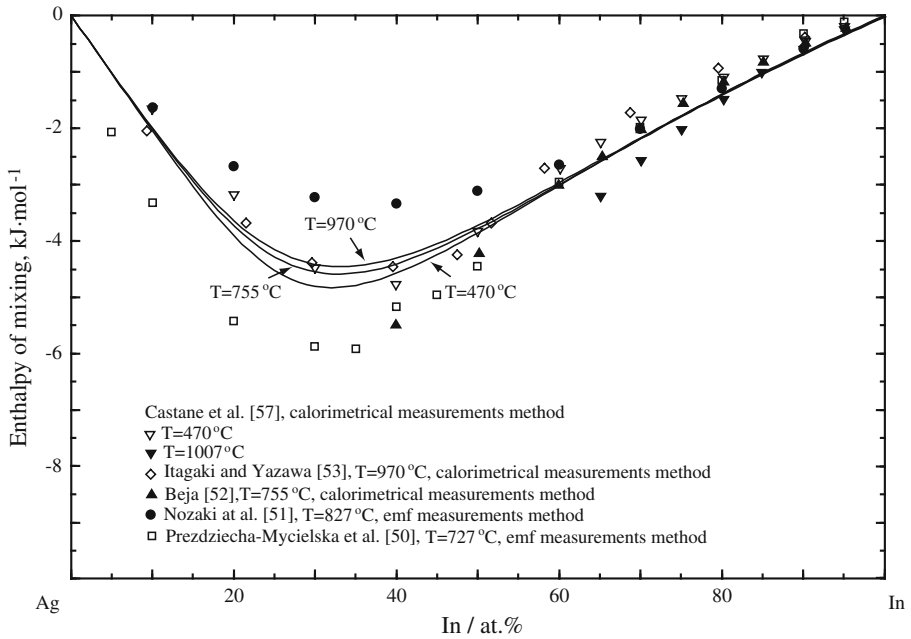

Fig. 9 Calculated enthalpy of mixing of liquid phase at 470, 755 and 970 °C of Ag-In system compared with experimental data[50-53,57]

et al.[105,106] A detailed description of the MQMPA and its associated notation are given in refs.[105,106]

4. Experimental Procedures

Mg-Sn-Ag ternary alloys were prepared with pure Mg (99.8 wt.%), Sn (99.9 wt.%), and Ag (99.9 wt.%) from Alfa Aesar and melted in a frequency induction furnace under high purity argon atmosphere. In order to minimize the interaction of the samples with the crucibles, Ta cubic-shaped crucibles were made using Ta foil (99.5 wt.% purity, 0.15 mm thickness). Each alloy was remelted three times in its crucible in order to obtain a homogeneous alloy; the melting loss was less than 5 wt.% for each sample. Mg-Sn-Ag samples were then sealed into quartz capsules under argon atmosphere and equilibrated at 415 °C for 20 days and at 350 °C for 35 days,

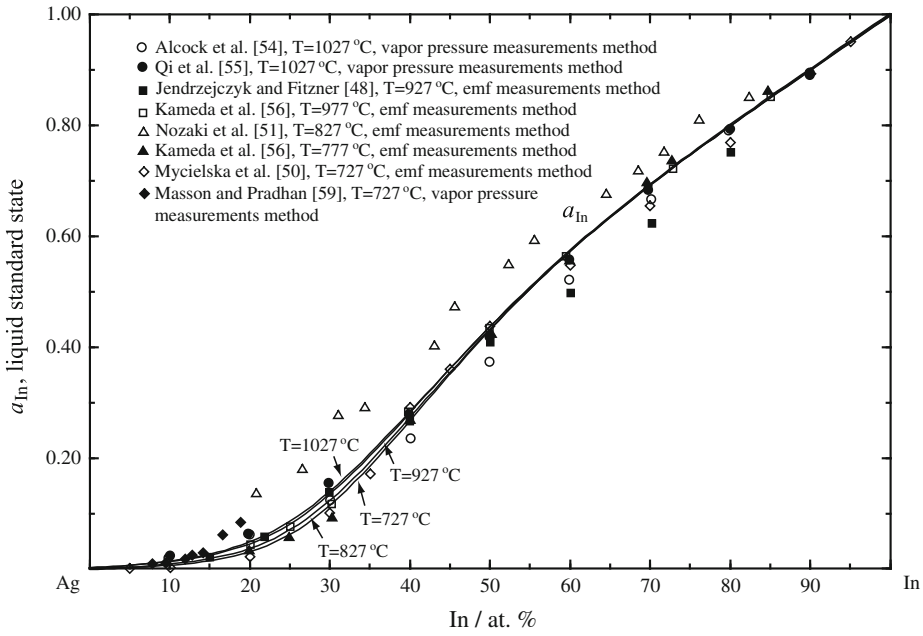

Fig. 10 Calculated activity of In in the liquid phase in the temperature range of 727 to 1027 °C compared with experimental data[48,50,51,54-56,59]

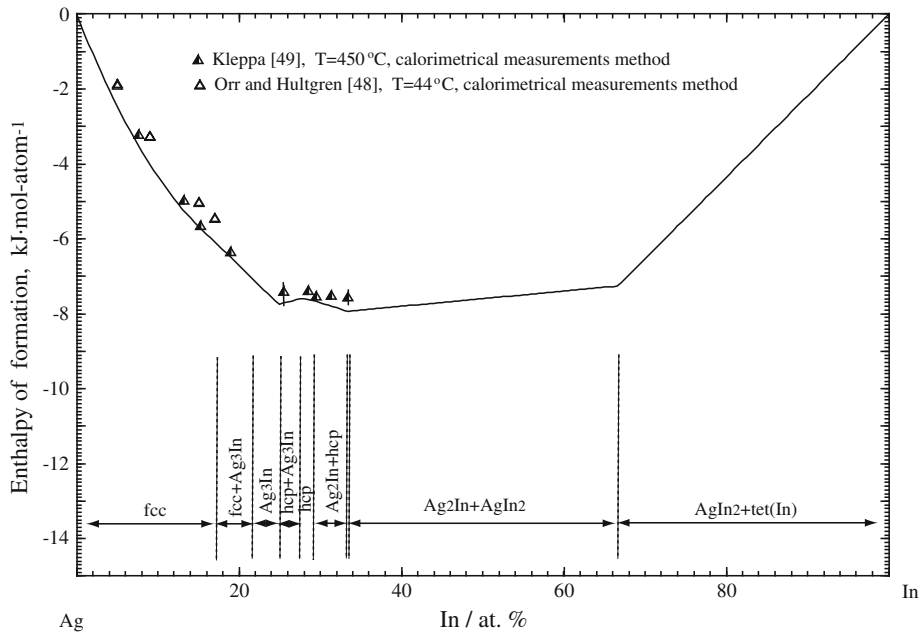

Fig. 11 Calculated heat formation of solid phases of Ag-In system at 25 °C compared with experimental data[49,58]

respectively. These temperatures were chosen because they correspond to the temperatures at which heat treatment is usually performed on Mg alloys. Quenching was carried out in water without breaking the quartz tubes. The alloys preparation was done at Concordia University

Electron probe microanalysis (EPMA) of the quenched samples was performed with the JEOL 8900 probe at McGill University using wavelength-dispersive spectrometry (WDS). An accelerating voltage of 15 kV was used with a 20 nA beam current, a spot size of 2 μm and counting times of 20 s on peaks and 10 s on backgrounds. Raw data were reduced with the PRZ correction using pure Mg, Sn, and Ag metal standards. The experimental error limit of EPMA measurement is about 0∼3 at.%.

Table 9 Calculated invariant reactions in the Ag-Sn system compared with experimental data

Reaction	Reaction type	Temperature (°C)	Composition (Sn at.%)			Reference
liquid + fcc ↔ hcp	Peritectic	724	19.5	11.5	13.0	[72]
		724	20.3	11.3	12.7	This work
liquid + hcp ↔ Ag_3Sn	Peritectic	480	49.6	22.8	25.0	[72]
		480	52.1	25.3	26.0	This work
liquid ↔ Ag_3Sn + bct (Sn)	Eutectic	221	96.2	25.9	99.91	[72]
		221	96.2	25.9	99.93	This work

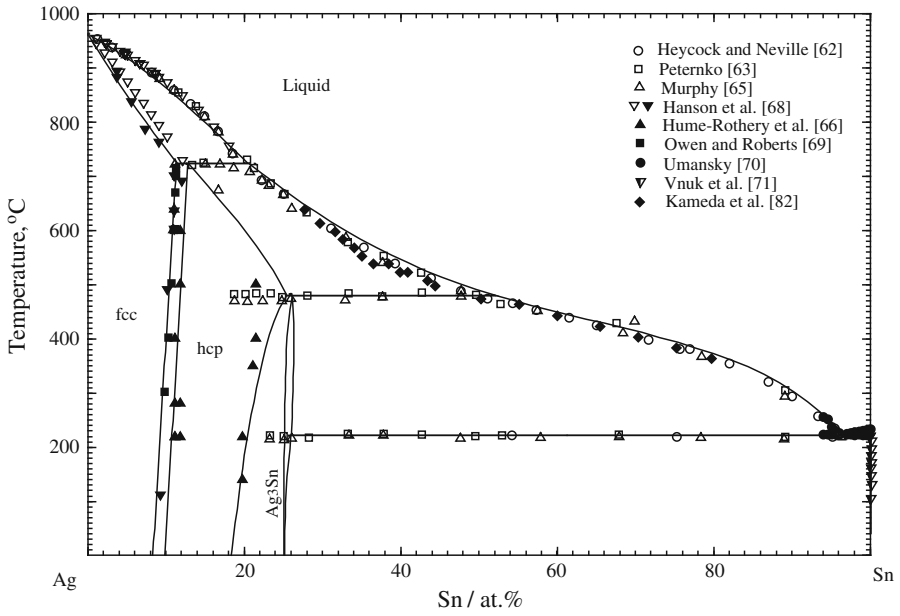

Fig. 12 Calculated phase diagram of Ag-Sn system compared with experimental data[62,63,65,66,68-71,82]

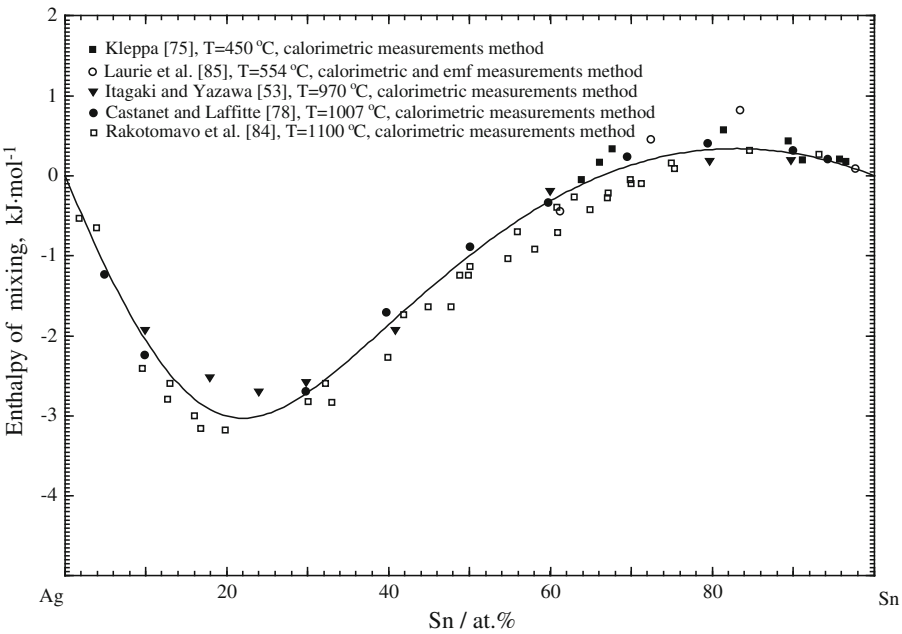

Fig. 13 Calculated mixing of enthalpy of liquid phase of Ag-Sn system at 1000 °C compared with experimental data[53,75,78,84,85]

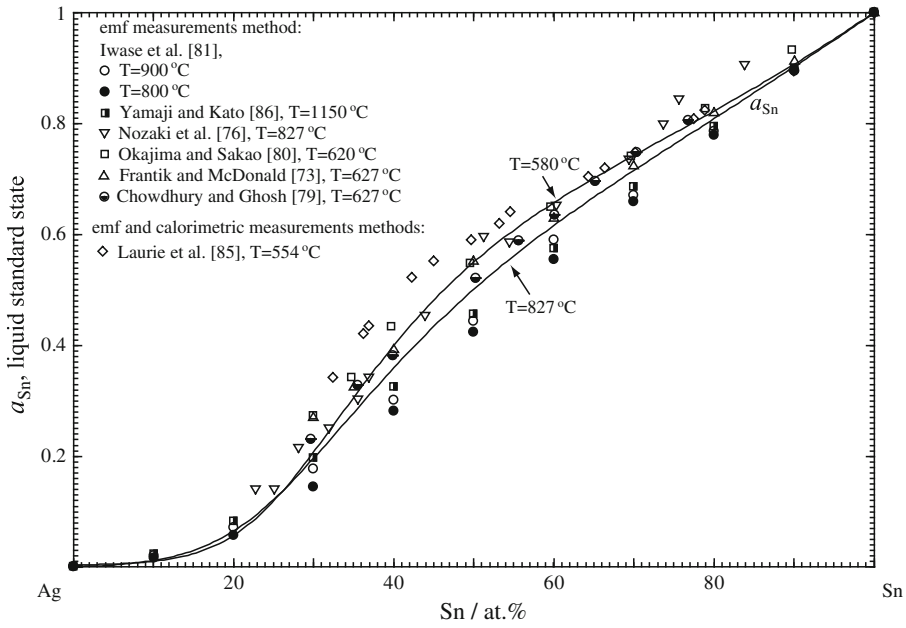

Fig. 14 Calculated activity of Sn in liquid Ag-Sn alloys at 827 and 580 °C compared with experimental data[73,76,79-81,85,86]

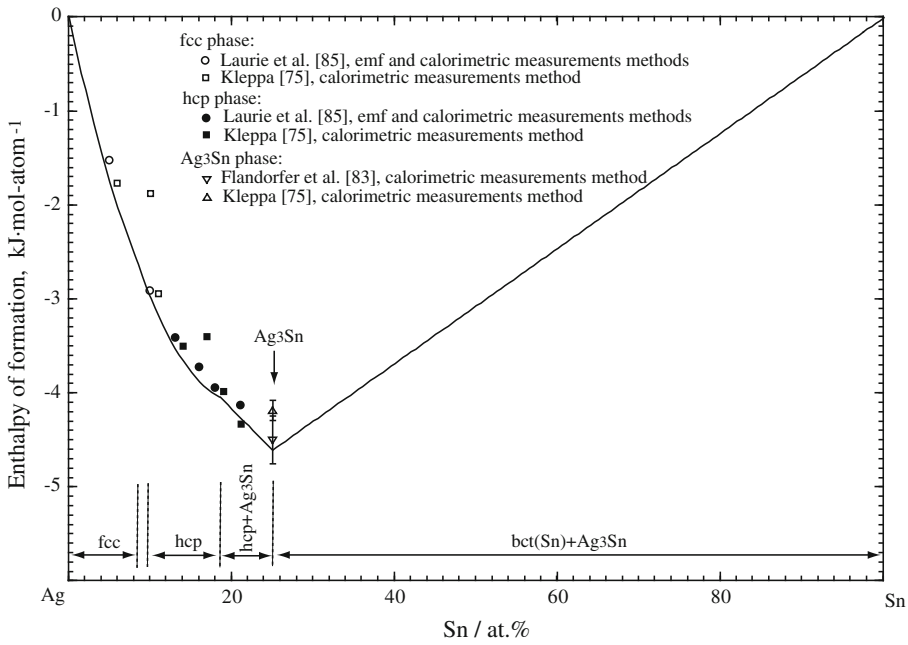

Fig. 15 Calculated enthalpy of formation of compounds of Ag-Sn system at 25 °C compared with experimental data[75,83,85]

Liquidus and polymorphic transformation temperatures were measured by differential scanning calorimetry (DSC) using the SETARAM instrumentation under a continuous flow of purified argon at Concordia University. Experiments were carried out by using sintered Al_2O_3 crucibles under flowing argon gas with heating and cooling rates of 5 °C/min. No reaction was observed between the samples and the sintered Al_2O_3 crucibles.

5. Experimental and Thermodynamic Optimization Results

5.1 Experimental Determination Results of the Mg-Sn-Ag System

Equilibrium compositions measured at 415 and 350 °C in the Mg-rich area of the Mg-Sn-Ag system are

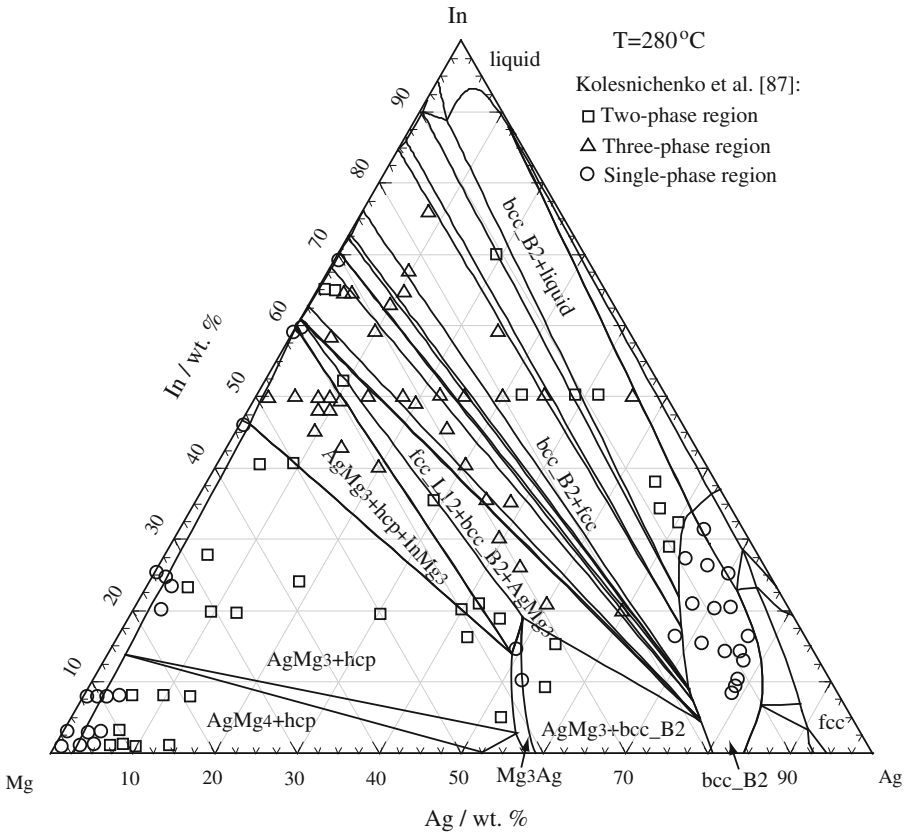

Fig. 16 Calculated isothermal section of Mg-Ag-In ternary system at 280 °C along with experimental data[87]

summarized in Table 3. Sums of elemental compositions are always close to 100 wt.% which indicates that Mg loss by evaporation was small. No ternary compound was found in the measured sections. The solubility of Ag in Mg_2Sn at 415 and 350 °C is very limited (less than 0.1 at.%). The solubility of Sn in Mg_3Ag at 415 and 350 °C is about 2.5 to 3 at.%. With Sn additions, the ternary equilibrium hcp (Mg) + Mg_2Sn + Mg_3Ag was observed in both isothermal sections. On the other hand, in the Mg-Ag system, no binary equilibrium involving hcp (Mg) + Mg_3Ag was detected. Typical ternary Mg-Sn-Ag alloys are shown in the back-scattered electron (BSE) images of Fig. 1. The constituted phases in annealed samples were examined with XRD technique, and the selected XRD patterns of samples Mg50-Sn20-Ag30 and Mg80-Sn10-Ag10 are shown in Fig. 2. As shown in Fig. 1(c), the amount of hcp (Mg) phase is small in comparison with the Mg_2-Sn and Mg_3-Ag phases. The weak diffraction patterns of the hcp (Mg) phase were observed in the XRD results as shown in the Fig. 2(b). These results are self-consistent.

The ternary isoplethal sections with the constant Sn of 10 and Ag of 30 (at.%) were measured in the present work by DSC technique. The DSC curve of the Mg80-Sn10-Ag10 alloy is shown in Fig. 3. Three strong exothermic peaks and one weak peak were observed in the cooling spectrum, which were well repeated during heating with two endothermic peaks and one weak liquid peak. All the thermal signals obtained from DSC measurements are listed in Table 4.

5.2 Thermodynamic Optimization Results

5.2.1 The Ag-Mg System. The calculated phase diagram of the Ag-Mg binary system is shown in Fig. 4 along with reported experimental data.[20-24,29-31] Ordering of the bcc_B2 (AgMg), Ag_3Mg and Mg_3Ag phases was treated with two sublattices as $(Ag, Mg)_m(Ag, Mg)_n$. Moreover, based on the results of phase transition and the solid solubility range of $Mg_{54}Ag_{17}$ reported by Kolesnichenko et al.[29] $Mg_{54}Ag_{17}$ was treated as a high temperature stable phase with a narrow solid solubility range, using a two sublattice model, $(Ag, Mg)_{17}(Mg)_{54}$, in the present work. The calculated temperature of the eutectic reaction liquid ↔ $Mg_{54}Ag_{17}$ + hcp is 471 °C, which is in good agreement with the temperature of 472 °C measured by Kolesnichenko et al.[29] All the invariant reactions of the calculated Ag-Mg phase diagram are listed in Table 5.

The calculated enthalpy of mixing of the liquid phase at 1050 °C is presented in Fig. 5 and compared with the experimental data of Kawakami,[32] which show a minimum near $x_{Mg} = 0.5$. Consequently in the present work, the coordination numbers for short-range ordering in the liquid solution were fixed as$Z^{Ag}_{AgMg} = 7$and $Z^{Mg}_{AgMg} = 7$(as listed in Table 6). The calculated ΔG^{xs}_{Mg} versus $(1\text{-}x_{Mg})^2$ of the liquid

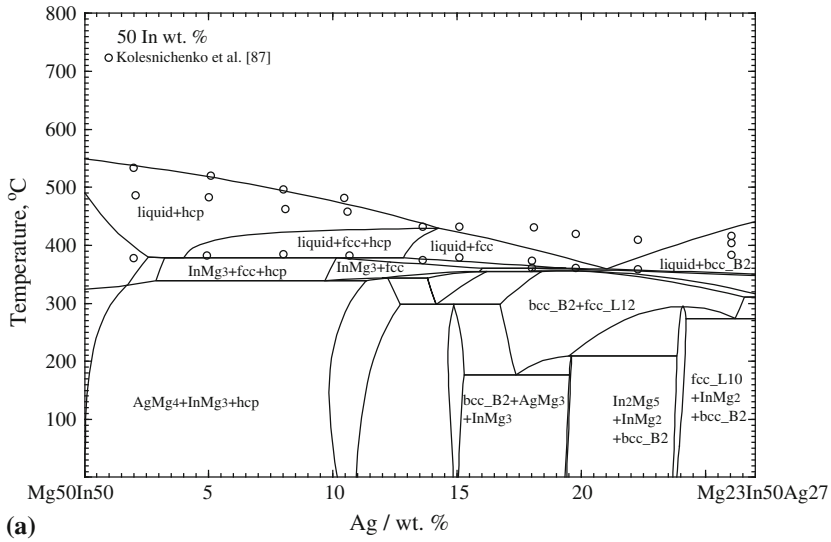

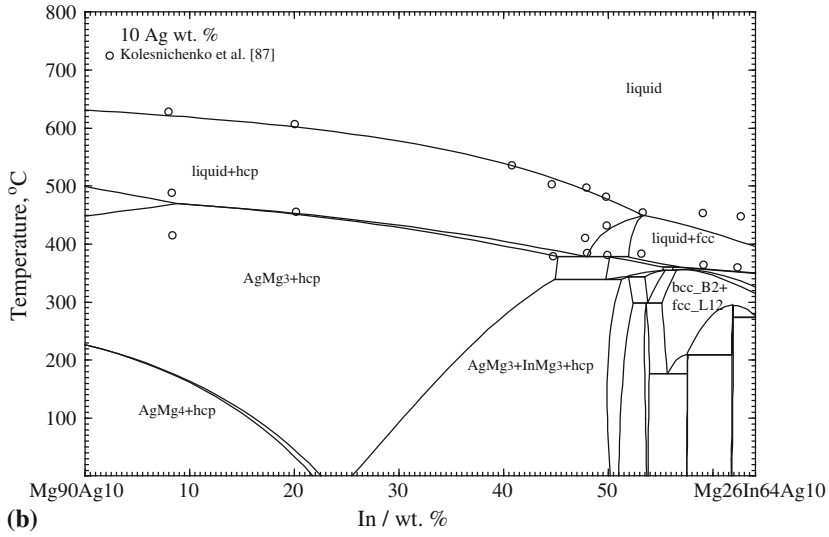

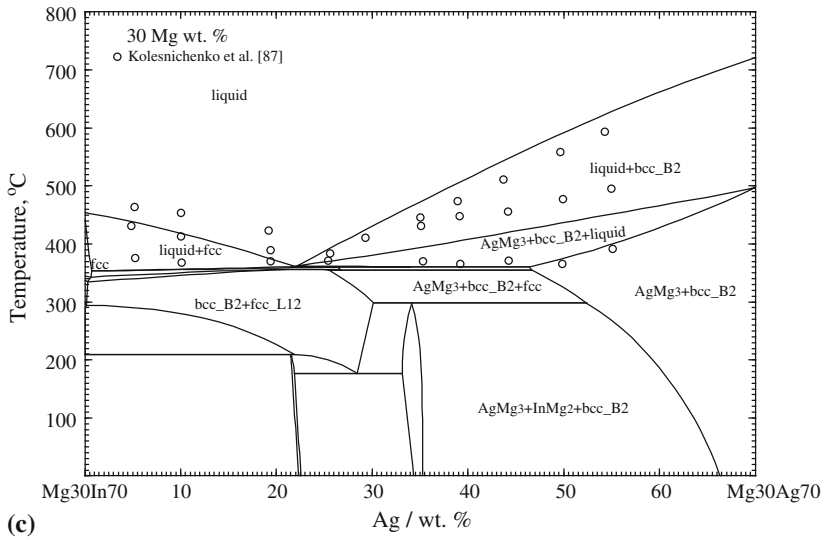

Fig. 17 Calculated ternary isoplethal sections of the Mg-Ag-In system at (a) 50 In, (b) 10 Ag, and (c) 30 Mg (wt.%) along with the experimental data[87]

Table 10 Calculated invariant reactions in the liquidus projection of the Mg-Ag-In ternary system

Label	T (°C)	Reaction	Composition of liquid (at. %)		
			In	Mg	Ag
E1	145	L ↔ tet(In) + bcc_B2 + In_2Ag	1.08	2.84	96.08
U1	377	L + hcp ↔ $AgMg_3$ + fcc	18.97	70.09	10.94
U2	360	L + $AgMg_3$ ↔ fcc + bbc_B2	22.36	66.64	11.00
U3	162	L + $InAg_2$ ↔ In_2Ag + hcp	95.58	0.09	4.33
U4	161	L + hcp ↔ bcc_B2 + In_2Ag	95.56	0.20	4.24
U5	156	L + fcc ↔ tet(In) + bcc_B2	96.69	2.17	1.14
U6	557	L + bcc_A2 ↔ hcp_A3 + bcc_B2	39.70	1.07	56.23
U7	468	L + $Ag_{17}Mg_{54}$ ↔ hcp_A3 + $AgMg_3$	0.86	83.09	16.05
P1	792	L + fcc ↔ bcc_A2 + bcc_B2	10.20	12.55	77.25
P2	491	L + $Ag_{17}Mg_{54}$ ↔ hcp_A3 + $AgMg_3$	0.54	78.36	21.10

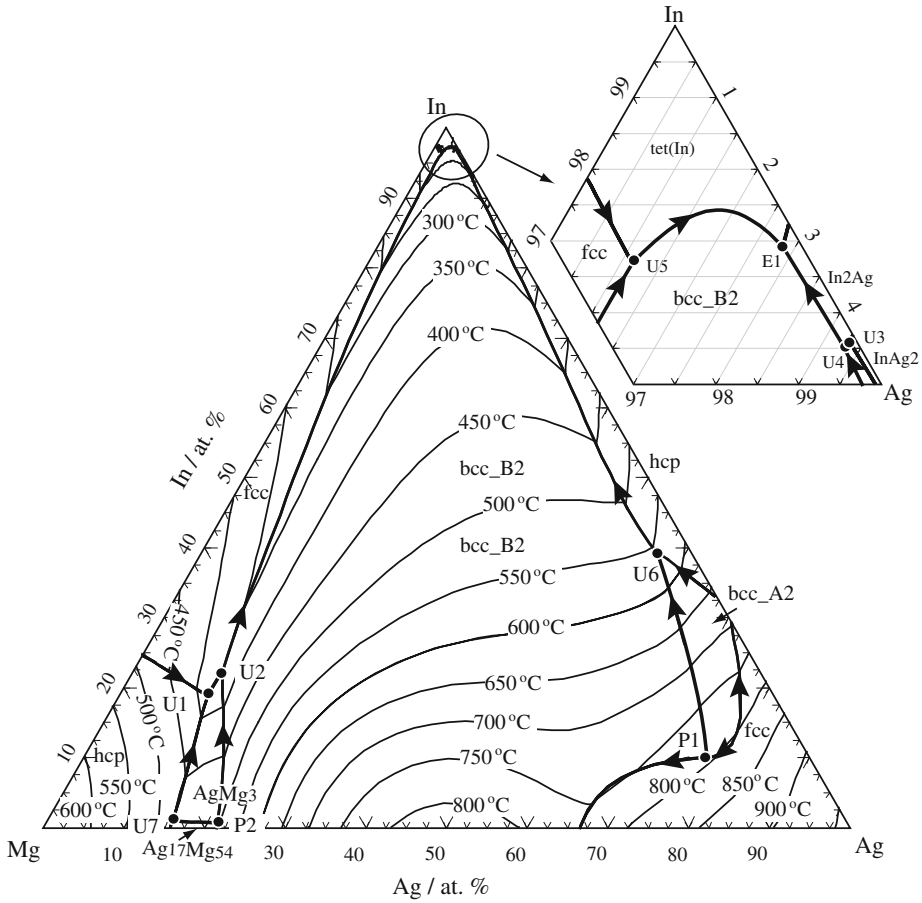

Fig. 18 Calculated liquidus projection of the Mg-Ag-In ternary system

phase at 1400 °C, along with the experimental data of Gran et al.[33] are depicted in Fig. 6. The calculated enthalpy of formation of the solid phases at 25 °C is shown in Fig. 7 together with the experimental data.[31,34-36]

As shown in the figures, our calculated results are in good agreement with experimental data. All the thermodynamic parameters used in the present study are listed in Tables 6 and 7.

5.2.2 The Ag-In System. The calculated phase diagram of the Ag-In binary system is shown in Fig. 8 along with the experimental data.[39,43,47,48] The bcc, fcc, hcp, $AgIn_2$, Ag_2In, Ag_3In phases were taken into account according to

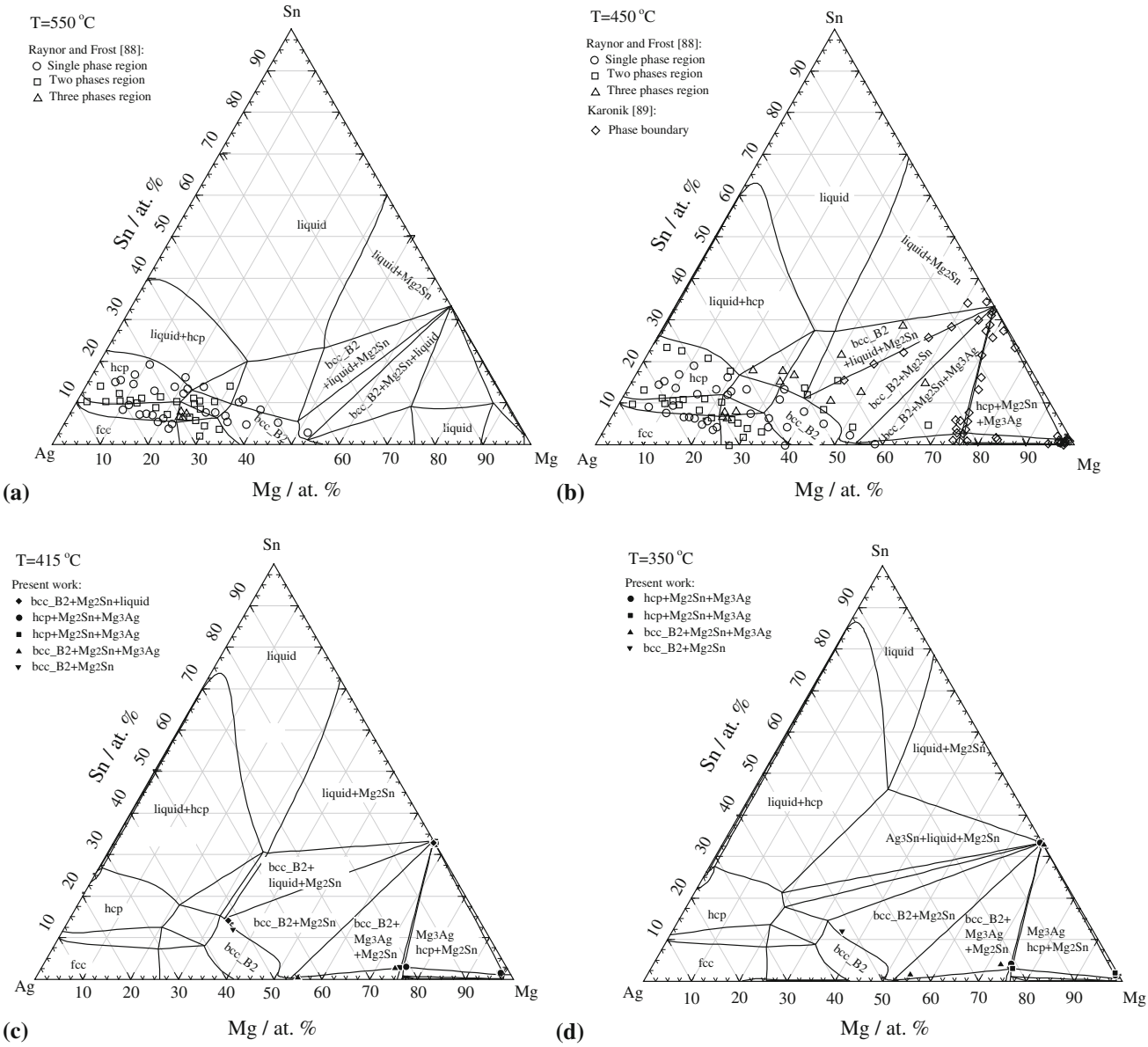

Fig. 19 Calculated isothermal sections of the Mg-Ag-Sn ternary system at (a) 550 °C, (b) 450 °C, (c) 415 °C, and (d) 350 °C along with experimental data[88,89]

the experimental results reported above. The Ag_2In phase was treated with a two sub-lattice model as (Ag, In) $(Ag)_2$ to reproduce its solid solubility and crystal structure.

The Ag_3In phase was calculated to decompose at 187 °C following the peritectoid reaction hcp + fcc ↔ Ag_3In, which is identical to the temperature measured by Weibke and Eggers[39] and Campbell and Wagemann[43] All the invariant reactions in the calculated phase diagram of Ag-In binary system are listed in Table 8.

The calculated enthalpies of mixing of the liquid phase at 470, 755, 970 °C are shown in Fig. 9 along with experimental data.[50-53,57] As shown in the figure, data obtained by direct calorimetric measurements[52,53,57] are in reasonable agreement with each other. However, data derived from emf measurements[50,51] do not agree very well with the data obtained by direct calorimetric measurements. Therefore, priority was given to the later during the optimization. The calculated activities of In in the liquid phase, collected between 727 and 1027 °C, are shown in Fig. 10 together with the experimental data discussed above.[48,50,51,54-56,59] The calculated enthalpies of formation of the solid phases at 25 °C are shown in Fig. 11 along with the experimental data of Kleppa[49] and Orr and Hultgren.[58]

As we can see from the figures, our calculated results are in good agreement with experimental data. All the parameters of the thermodynamic models are listed in Tables 6 and 7.

5.2.3 The Ag-Sn System. The calculated phase diagram of the Ag-Sn binary system is shown in Fig. 12 along with experimental data.[62,63,65,66,68-71,82] According to our

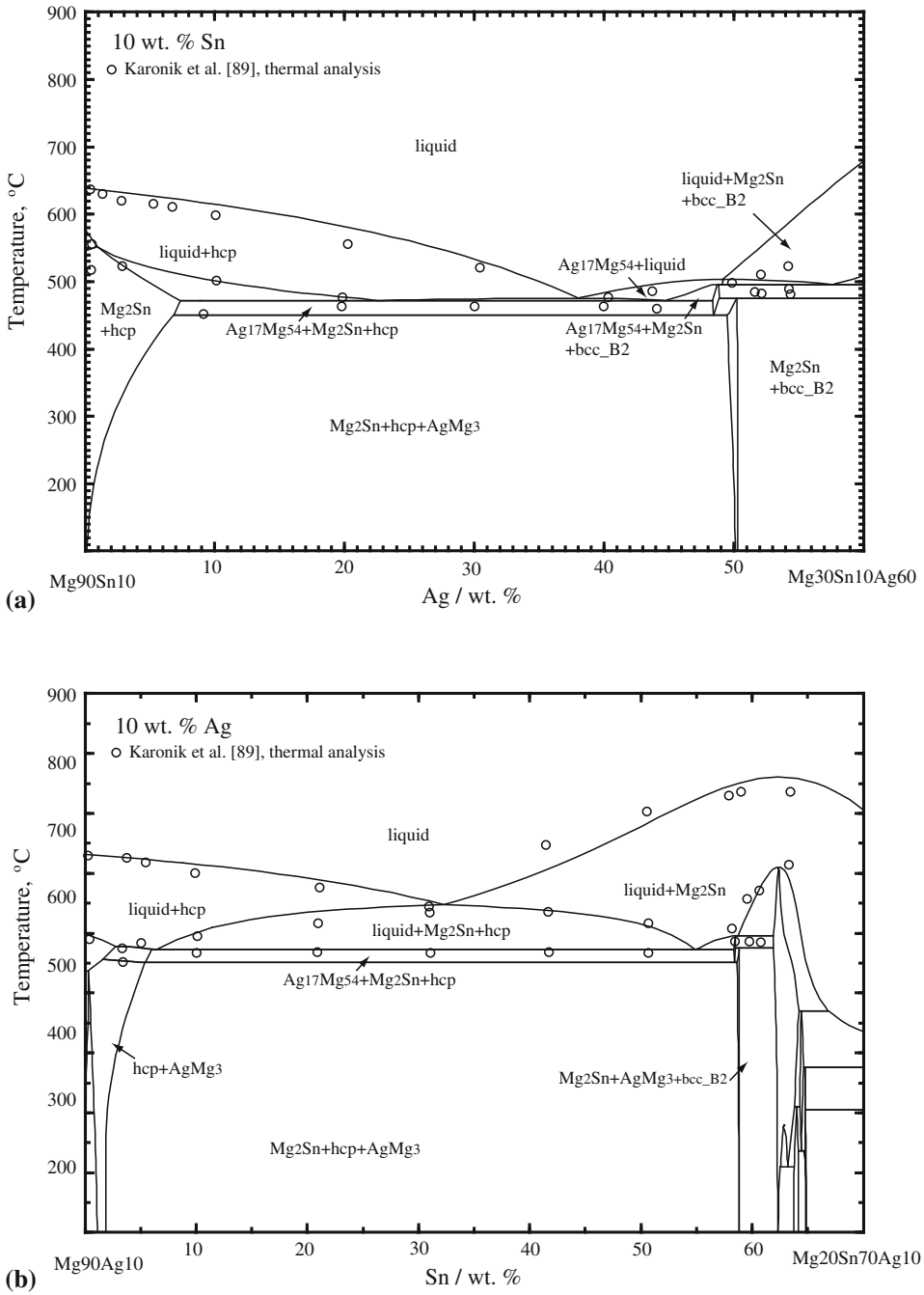

Fig. 20 Calculated isoplethal sections of the Mg-Ag-Sn system at (a) 10 Sn and (b) 10 Ag (wt.%) compared with experimental data[89]

calculations, the hcp phase is formed from the peritectic reaction liquid + fcc ↔ hcp at 724 °C, which is identical to the experimental data reported by Murphy.[65] The Ag_3Sn binary compound was treated as a solid solution with a two sub-lattice model as (Ag, Sn)$_3$ (Sn). It was calculated to form at 480 °C from the peritectic reaction liquid + hcp ↔ Ag_3Sn, which is in good agreement with experimental data.[63,65] All our calculated invariant reactions along with the compiled experimental data are listed in the Table 9.

The calculated enthalpy of mixing of the liquid phase at 1000 °C, the calculated activity of Sn in the liquid phase, and the calculated enthalpies of formation of the solid phases at 25 °C are shown along with experimental data in Fig. 13, 14, and 15, respectively. As we can see, all the data are in a reasonable agreement with each other and our optimization results agree well with the reported experimental data. All the optimized thermodynamic parameters are listed in Tables 6 and 7.

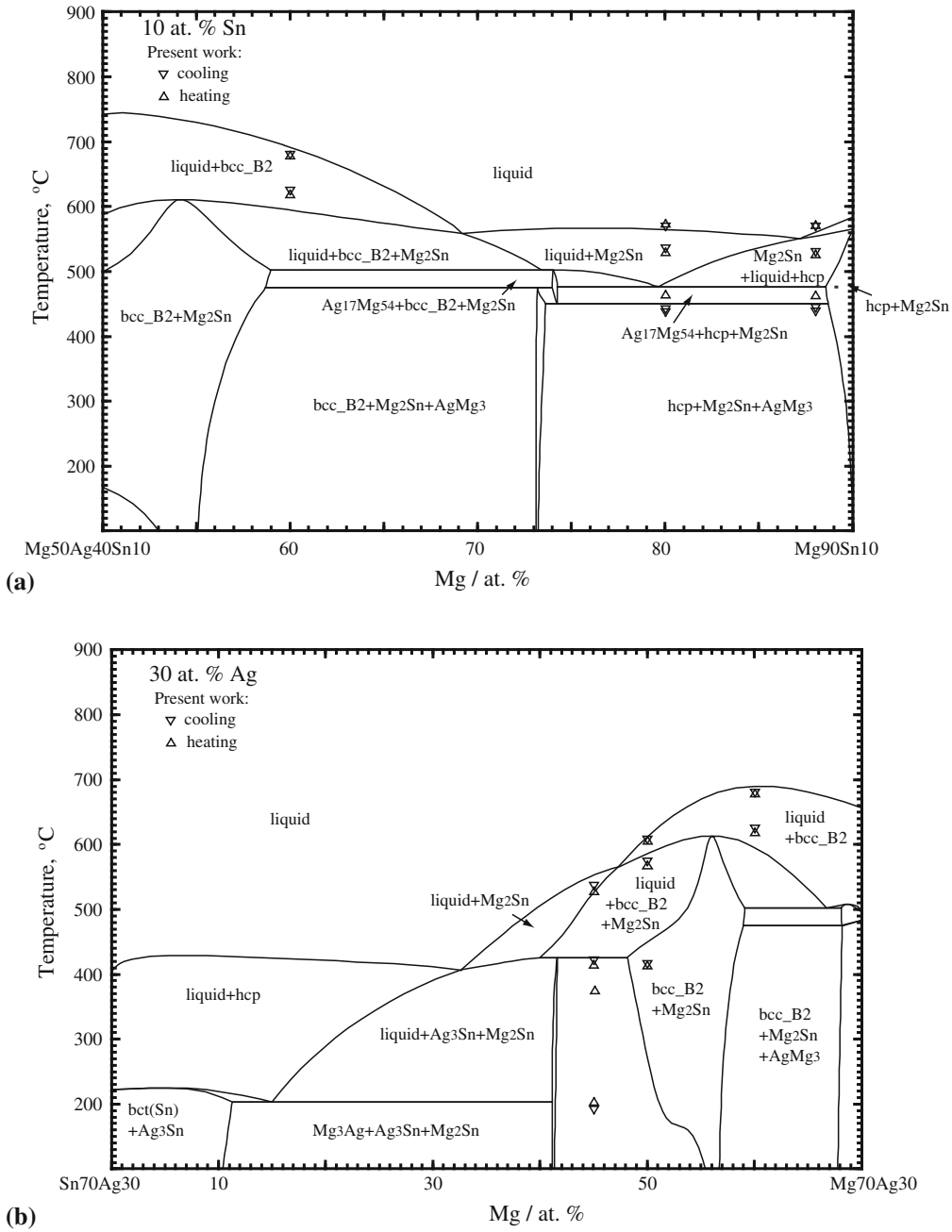

Fig. 21 Calculated isoplethal sections of the Mg-Ag-Sn system at (a) 10 Sn and (b) 30 Ag (at. %) along with experimental data from present work

5.2.4 The Mg-Ag-In System. The Mg-In binary system was optimized in our previous work[97] and the Ag-Mg, and Ag-In in this one. The liquid phases of the Mg-In, Ag-Mg, and Ag-In binary systems have totally different thermodynamic properties; as a result, ternary parameters of the liquid phase of Mg-Ag-In system were modeled with the symmetric Kohler-like[107] approximation in the MQMPA.

The calculated isothermal section at 280 °C and the three ternary isopleths are shown in Figs. 16 and 17, respectively, along with experimental data[87] As shown in Fig. 16, the calculated results are in a reasonable agreement with experimental data. However, the solubility limits of In and Ag in the terminal hcp (Mg) phase, as reported by Kolesnichenko,[87] are different from the compiled data on the Mg-Ag binary system.[19] Consequently, new experimental data appear to be necessary here to resolve this issue.

The calculated liquidus projection of the Mg-Ag-In ternary system is shown in Fig. 18 and the calculated invariant reactions are listed in Table 10. All the optimized thermodynamic parameters are listed in the Tables 6 and 7.

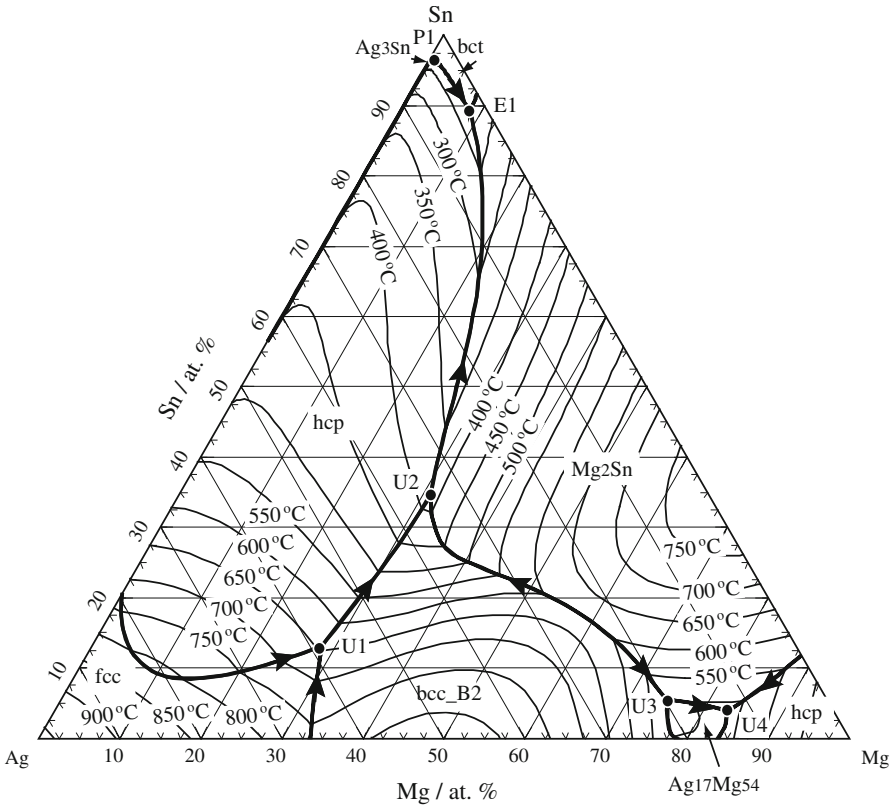

Fig. 22 Calculated liquidus projection of the Mg-Ag-Sn ternary system

Table 11 Calculated invariant reactions in the liquidus projection of the Mg-Sn-Ag ternary system

			Composition of liquid (at.%)		
Label	**T (°C)**	**Reaction**	**Mg**	**Ag**	**Sn**
P1	221	L + hcp ↔ bct + Ag_3Sn	0.01	3.85	96.13
E1	200	L ↔ bct + Mg_2Sn + hcp	8.66	2.18	89.16
U1	641	L + fcc ↔ hcp + bcc_B2	28.39	58.46	13.15
U2	382	L + bcc_B2 ↔ hcp + Mg_2Sn	30.99	34.34	34.67
U3	503	L + bcc_B2 ↔ $Mg_{54}Ag_{17}$ + Mg_2Sn	74.87	19.73	5.39
U4	476	L ↔ hcp + $Mg_{54}Ag_{17}$ + Mg_2Sn	83.07	13.06	3.87

5.2.5 The Mg-Ag-Sn System. All the available data from Raynor and Frost,[88] Karonik et al.[89] and our current experimental data were taken into account in the present optimization. Since the liquid phases of the Ag-Mg, Ag-Sn, and Mg-Sn binary systems have totally different thermodynamic properties, the symmetric Kohler-like[107] extrapolation method was used for optimizing ternary liquid parameters of the Mg-Ag-Sn system within the MQMPA.

The calculated isothermal sections of the Mg-Ag-Sn ternary system are shown in Fig. 19 (a)-(d) along with experimental data from Raynor and Frost,[88] Karonik et al.[89] and our new experimental data. The calculated ternary isoplethal sections with constant Sn of 10 and Ag of 10 (wt.%) are depicted in Fig. 20 together with the experimental data of Karonik et al.[89] The calculated ternary isopleths with constant value of 10 Sn and 30 Ag at.%, in comparison with the current experimental data, are shown in Fig. 21. As it can be seen, our calculated results are in reasonable agreement with the experimental values. The calculated liquidus projection of the Mg-Ag-Sn system is shown in Fig. 22 and the calculated invariant reactions are listed in Table 11. All the optimized thermodynamic parameters are listed in the Tables 6 and 7.

5.2.6 The Ag-In-Sn System. The In-Sn binary system was optimized in our previous work.[97] Zivkovic et al.[108] performed a comparative thermodynamic study of the Ag-In-Sn system and pointed out that the Toop-like model[107] is the most accurate method to calculate ternary liquid mixing parameters assuming Ag as an asymmetric component; Kohler and Toop[107] extrapolation techniques were

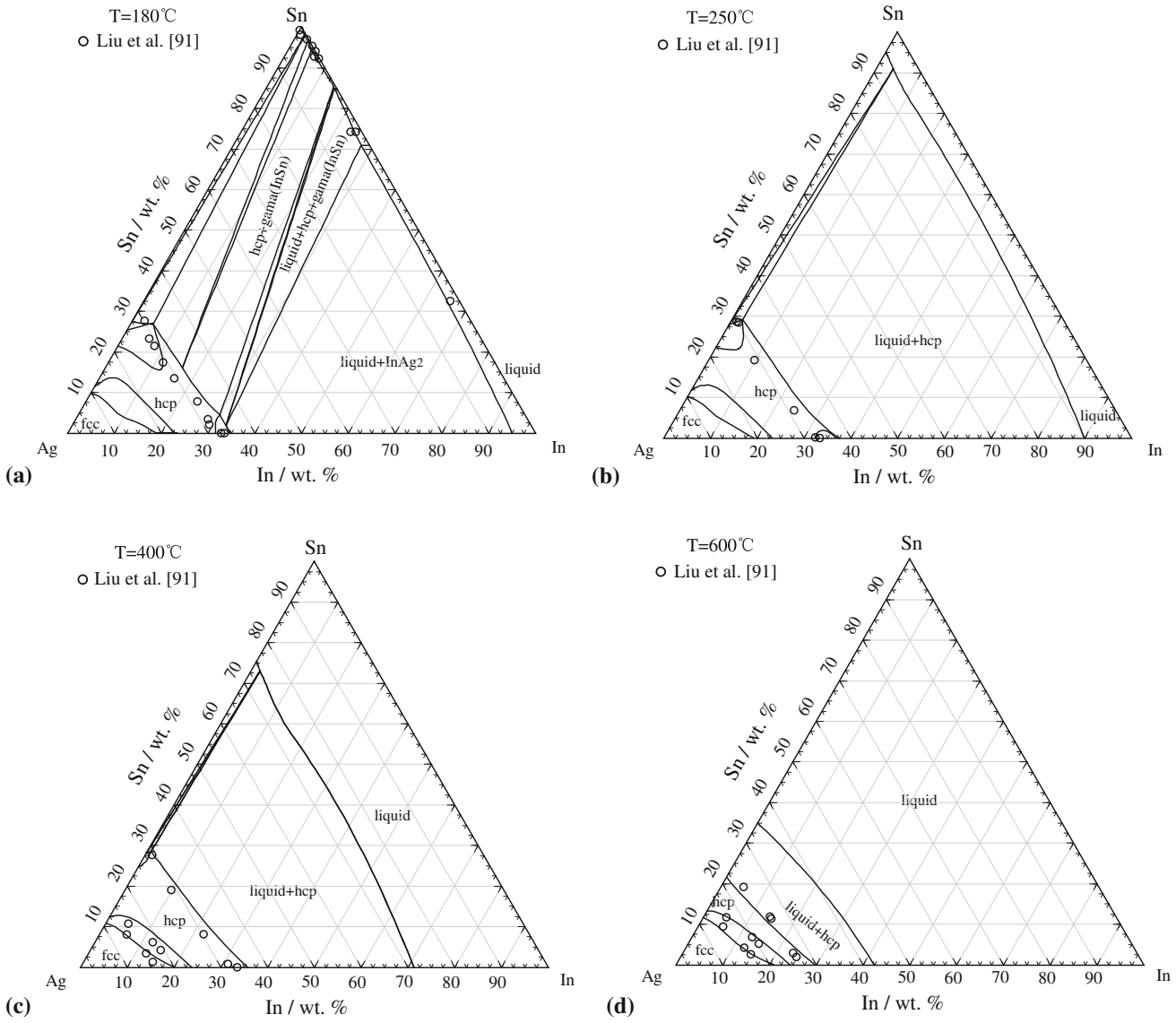

Fig. 23 Calculated isothermal sections of the Ag-In-Sn ternary system at (a) 180 °C, (b) 250 °C, (c) 400 °C, and (d) 600 °C along with experimental data[91]

both tested and Toop-like was found to be the best method to model the ternary liquid phase, which is in agreement with the suggestion from Zivkovic et al.[108]

The calculated isothermal sections at 180, 250, 400, and 600 °C and isoplethal sections are shown in Fig. 23 and 24, respectively, along with experimental data.[91] Comparison of the measured[94] and calculated enthalpy of mixing of the liquid phase with different In/Sn atomic ratios is presented in Fig. 25. As it can be seen, the calculated results agree relatively well with experimental data. All the thermodynamic parameters used are listed in the Tables 6 and 7.

5.2.7 The Mg-Sn-Ag-In System. Phase equilibria in the Mg-rich portion of the Mg-Sn-Ag-In quaternary system at 300 and 450 °C were investigated by Kolesnichenko et al.[109] by electrical conductivity, optical microscopy, and XRD. In the present optimization, the excess Gibbs energy contribution from the binary and ternary subsystems of the Mg-Sn-Ag-In quaternary system was interpolated using the method introduced by Pelton and Chartrand.[105] The same method and notation were used in the present work, and no additional model parameters were added. The calculated isothermal sections at 300 and 450 °C are shown in Fig. 26 along with the experimental data reported by Kolesnichenko et al.[109] As we can see, the current optimization gives satisfactory results when compared with experimental data.

Solidification calculations with the Scheil cooling technique for Mg96Sn3Ag1, Mg95Sn3Ag1In1, Mg93Sn6Ag1, and Mg92Sn6Ag1In1 (wt.%) alloys are shown in Fig. 27 (a-d). As depicted in Fig. 27 (a) and (c), the secondary $Mg_{54}Ag_{17}$ phase will appear in the final solidification microstructure of Mg-Sn based alloys with addition of 1

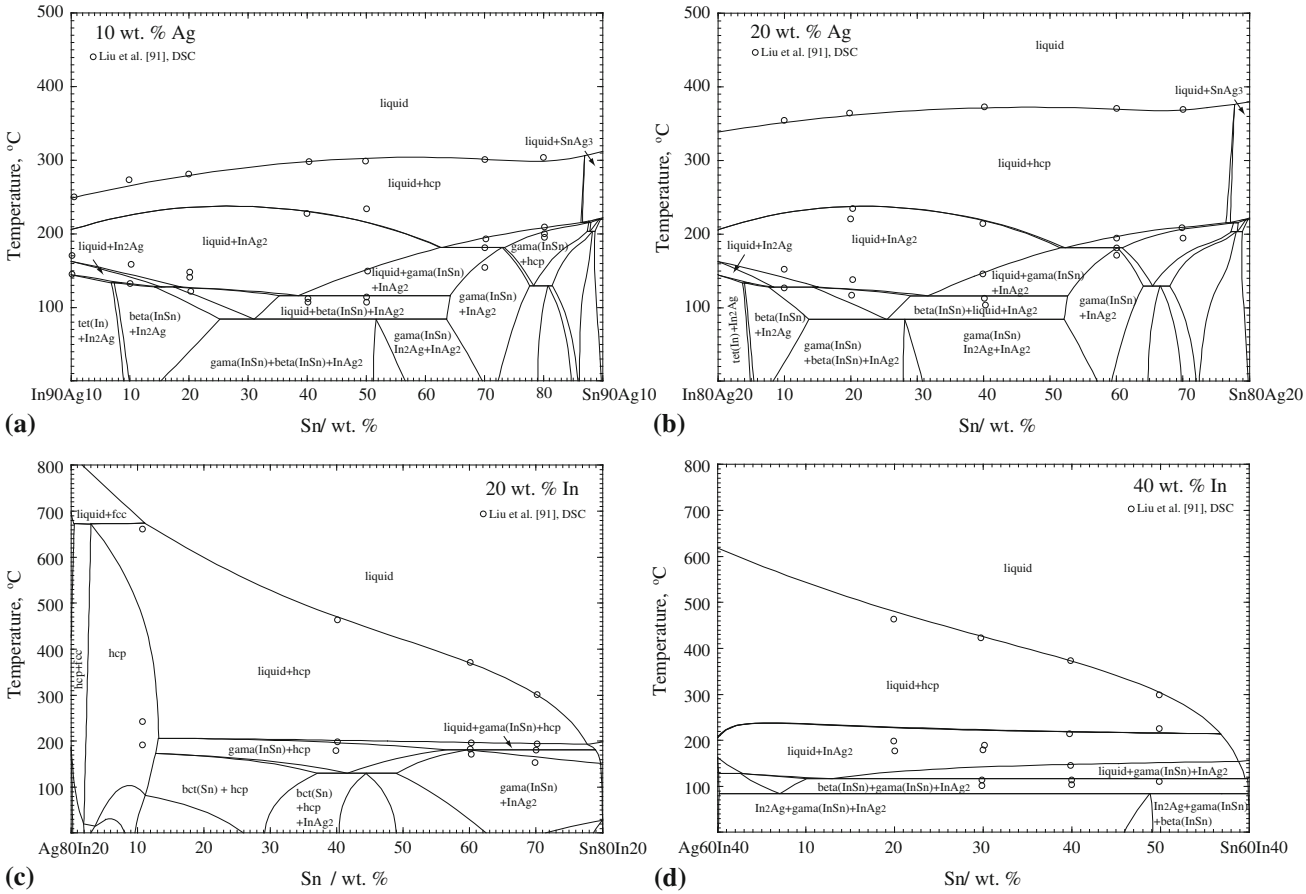

Fig. 24 Calculated isoplethal sections of the Ag-In-Sn system at (a) 10 Ag, (b) 20 Ag, (c) 20 In, (d) 40 In (wt.%) compared with experimental data[91]

wt.% Ag, which may improve mechanical properties. Compared to Ag addition alone, the combined addition of Ag and In (Fig. 27 (b) and (d)) gives some promising indications, more secondary precipitates, to improve the mechanical properties of Mg-Sn based alloys.

6. Discussions and Conclusions

Phase relations in the Mg-rich portion of the Mg-Sn-Ag system at 350 and 415 °C were determined by the quenching method, XRD, and EPMA. No ternary compound was found in the isothermal sections. The solid solubility of Ag in Mg_2Sn at 350 and 415 °C is very limited, less than 0.1 at.% (Since these values are within the error limits of the EPMA measurements, the solubilities are considered negligible), while the solubility of Sn in Mg_3Ag is quite large as 3±0.5 at.%, which is in good agreement with the experimental data reported by Karonik et al.[89] The ternary isoplethal sections with constant value of 10 Sn and 30 Ag at.% for Mg-Sn-Ag ternary system were also determined by DSC measurements.

A critical evaluation and thermodynamic assessment of the Ag-Mg, Ag-In and Ag-Sn binary systems, Mg-Ag-In, Mg-Ag-Sn and Ag-In-Sn ternary systems, and Mg-Sn-Ag-In quaternary system was carried out by the CALPHAD method. The Gibbs energy of the liquid phase was optimized with the Modified Quasichemical Model in pair approximation (MQMPA) and the solid solutions and intermetallic compounds were described with the sub-lattice model.

For the Ag-Mg binary system, ordering of the bcc (bcc_A2 and bcc_B2) and fcc (fcc_A1 and fcc_L12) phases was modeled with two sublattices and the symmetry of the crystal structure was taken in consideration. Moreover, all the phases and solid solubility limits reported in previous works were considered. $AgMg_3$ and $Mg_{54}Ag_{17}$ were also modeled with distinct sublattices according to their crystal structures in contrast with Lim et al.,[30] who treated them as single phases. Our optimized phase diagrams and thermodynamic properties are in better agreement with experimental data than Lim et al.,[30] especially for the description of the solidus curve of hcp(Mg) above the eutectic temperature (see Fig. 28) which is very important for the investigation of Mg alloys.

Although the thermodynamic optimization of the Ag-In binary system was carried out numerous times,[49,91] it still lacks accuracy. For instance, the high temperature stable phases bcc_A2, and $InAg_3$ were always ignored. In the

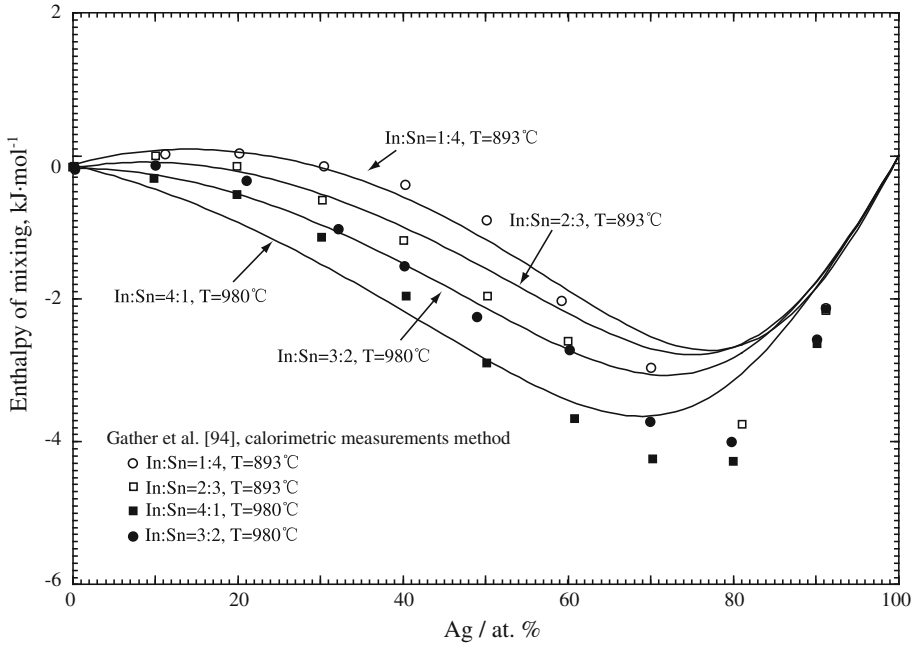

Fig. 25 Measured and calculated enthalpy of mixing of the Ag-In-Sn liquid alloys for different In/Sn atomic ratios[94]

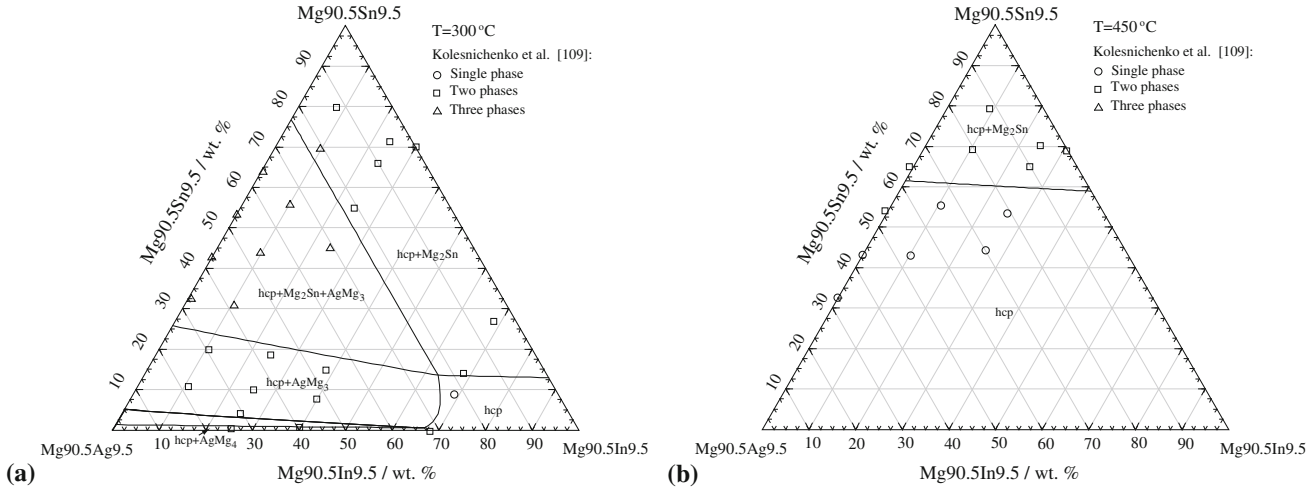

Fig. 26 Calculated isothermal sections of the Mg-Sn-Ag-In ternary system at (a) 300 °C and (b) 450 °C along with experimental data[109]

present work, after a critical evaluation of all the available experimental data, a strict thermodynamic re-optimization on the Ag-In binary system was performed using all experimental data, and all the existing phases were considered.

Phase relations in the Mg-Ag-In, Mg-Sn-Ag and Ag-In-Sn ternary systems were optimized using all available experimental data. As shown in Fig. 16, the solid solubility of In in $AgMg_3$ and bcc_B2 is quite important. However, due to the lack of experimental data, the ternary solid solubility of Ag in Mg-In compounds was not considered in the present work. Consequently, to obtain better optimization results for the Mg-Ag-In ternary system, new experimental data are clearly needed, especially at low Ag concentrations.

The current optimization of the Mg-Sn-Ag ternary system is in good agreement with the current experimental data and the previous ones.[88,89] The calculated liquidus projection (see Fig. 22) indicates the presence of a stable ternary peritectic reaction with a high Mg component at the end of the solidification process (see Fig. 27).

In the Ag-Sn-In ternary system, which is part of the lead-free solder thermodynamic database, experimental and

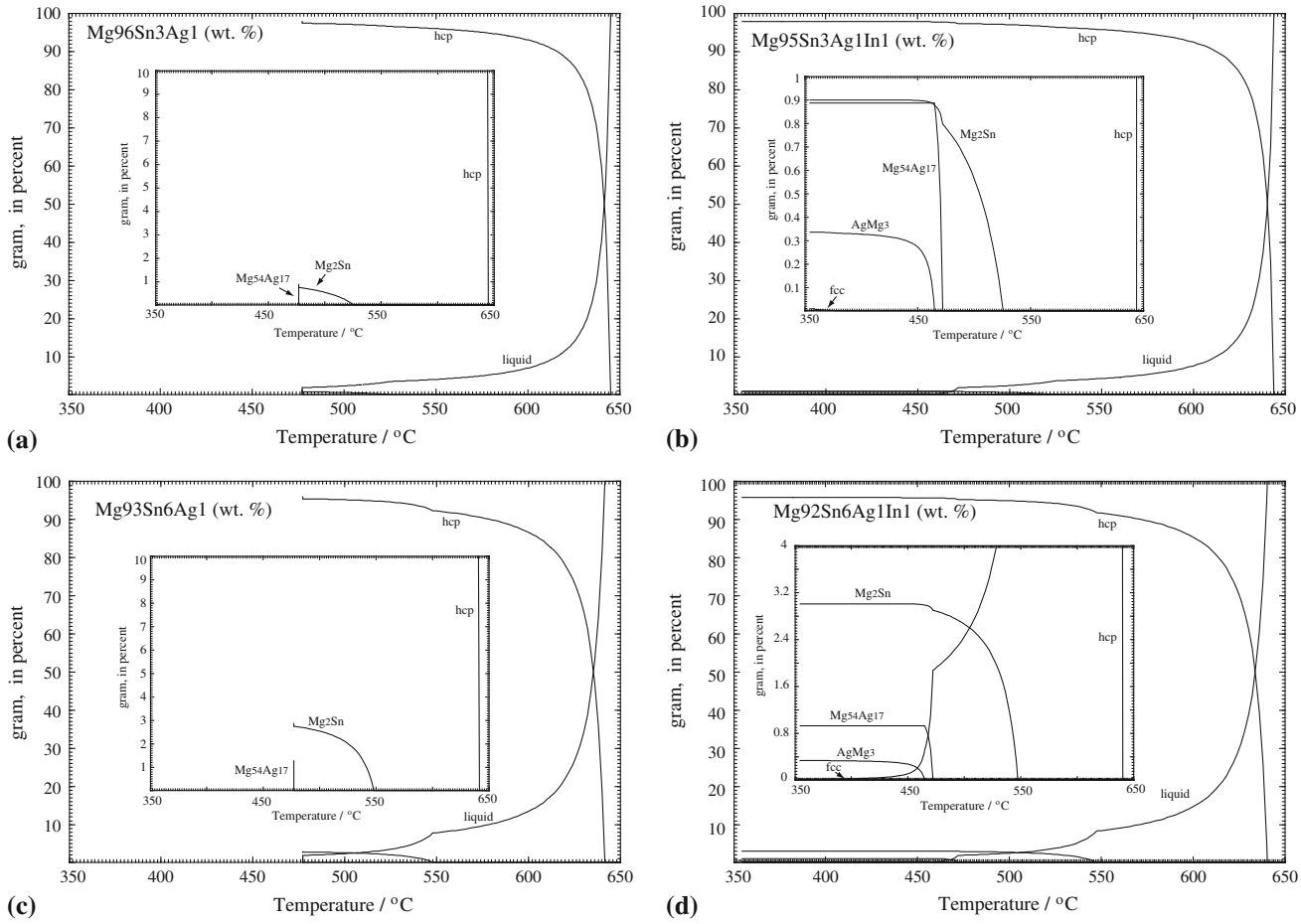

Fig. 27 Calculated solidification phase proportions (weight basis) using the Scheil cooling method for Mg-Sn-Ag and Mg-Sn-Ag-In alloys: (a) 96Mg3Sn1Ag, (b) 95Mg3Sn1Ag1In, (c) 93Mg6Sn1Ag, (d) 92Mg6Sn1Ag1In

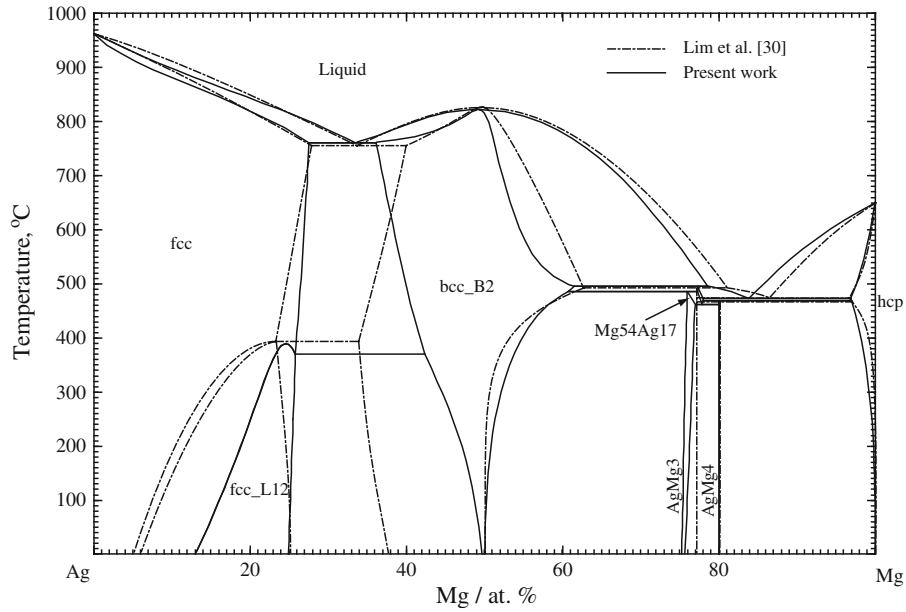

Fig. 28 Calculated phase diagram of the Ag-Mg system in the present work in comparsion with the previous optimization by Lim et al.[30]

thermodynamic data are quite numerous. In the present work, all these data are in good agreement with the current optimization.

By combining all these results with our previous thermodynamic optimization of the Mg-In-Sn ternary system,[97] a self-consistent thermodynamic database for the Mg-Sn-Ag-In quaternary system was constructed despite the limited experimental data[109] available. As shown in Fig. 27, solidification calculations with the Scheil cooling technique for the Mg-Sn based alloys with Ag and In additives give interesting indications to improve the mechanical properties of these alloys. With the combining addition of Ag and In to Mg-xSn (x = 3 or 6 wt.%) alloys, the final solidification microstructures become more complex, as they include secondary phases such as $Mg_{54}Ag_{17}$, Mg_3Ag, and fcc. The appearances of these secondary phases during the cooling process will improve grain refinement in Mg_2Sn and hcp phases.

A self-consistent thermodynamic database of the Mg-X (X: Ag, Ca, In, Li, Na, Sn, Sr, and Zn) multi-component system was constructed with the previously published results[97,110] and the present thermodynamic optimized results of the Mg-Sn-Ag-In quaternary system which shall help in the development of Mg alloys for industrial applications.

Acknowledgments

Financial support from General Motors of Canada Ltd. and the Natural Sciences and Engineering Research Council of Canada through the CRD grant program is gratefully acknowledged. The support in the experimental part from Mr. Tian Wang and Yi-Nan Zhang of Concordia University and Dr. Shi Lang from McGill University is acknowledged by the authors.

References

1. Y. Kojima, Platform science and technology for advanced magnesium alloys, *Mater. Sci. Forum*, 2000, p 3-18
2. M.A. Gibson, X. Fang, C.J. Bettles, and C.R. Hutchinson, The Effect of Precipitate State on the Creep Resistance of Mg-Sn Alloys, *Scripta Mater.*, 2010, **63**, p 899-902
3. D.H. Kang, S.S. Park, Y.S. Oh, and N.J. Kim, Effect of Nano-Particles on the Creep Resistance of Mg-Sn Alloys, *Mater. Sci. Eng. A*, 2007, **449-451**, p 318-321
4. T.A. Leil, Y.D. Huang, H. Dieringa, N. Hort, K.U. Kainer, J. Buršík, Y. Jirásková, K.P. Rao, Effect of Heat Treatment on the Microstructure and Creep Behavior of Mg-Sn-Ca Alloys, Mater. Sci. Forum, 2007, p 69-72
5. N. Hort, Y. Huang, T. Abu Leil, P. Maier, and K.U. Kainer, Microstructural Investigations of the Mg-Sn-xCa System, *Adv. Eng. Mater.*, 2006, **8**, p 359-364
6. T.A. Leil, N. Hort, W. Dietzel, C. Blawert, Y. Huang, K.U. Kainer, and K.P. Rao, Microstructure and Corrosion Behavior of Mg-Sn-Ca Alloys After Extrusion, *T. Nonferr. Metal. Soc.*, 2009, **19**, p 40-44
7. K. Van der Planken, Solution Hardening of Lead Single Crystals at Liquid Air Temperature, *J. Mater. Sci.*, 1969, **4**, p 927
8. C.L. Mendis, C.J. Bettles, M.A. Gibson, and C.R. Hutchinson, An Enhanced Age Hardening Response in Mg-Sn Based Alloys Containing Zn, *Mater. Sci. Eng. A*, 2006, **435-436**, p 163-717
9. C.L. Mendis, C.J. Bettles, M.A. Gibson, S. Gorsse, and R. Hutchinson, Refinement of Precipitate Distributions in an Age-Hardenable Mg-Sn Alloy Through Microalloying, *Phil. Magazin. Lett.*, 2006, **86**, p 443-456
10. T.T. Sasaki, K. Oh-ishi, T. Ohkubo, and K. Hono, Enhanced Age Hardening Response by the Addition of Zn in Mg-Sn Alloys, *Scripta Mater.*, 2006, **55**, p 251-254
11. S. Fang, X. Xiao, L. Xia, W. Li, and Y. Dong, Relationship Between the Widths of Supercooled Liquid Regions and Bond Parameters of Mg-Based Bulk Metallic Glasses, *J. Non-Cryst. Solids*, 2003, **321**, p 120-125
12. G. Liang, Synthesis and Hydrogen Storage Properties of Mg-Based Alloys, *J. Alloy. Comp.*, 2004, **370**, p 123-128
13. G. Ben-Hamu, D. Elizer, A. Kaya, Y.G. Na, and K.S. Shin, Microstructure and Corrosion Behavior of Mg-Zn-Ag Alloys, *Mater. Sci. Eng. A*, 2006, **435-436**, p 579-587
14. C.L. Mendis, K. Oh-ishi, and K. Hono, Enhanced age Hardening in a Mg-2.4 at. % Zn Alloy by Trace Additions of Ag and Ca, *Scripta Mater.*, 2007, **57**, p 485-488
15. H.T. Son, D.G. Kim, and J.S. Park, Effects of Ag Addition on Microstructures and Mechanical Properties of Mg-6Zn-2Sn-0.4Mn-Based Alloy System, *Mater. Lett.*, 2011, **65**, p 3150-3153
16. N. Saunders and A.P. Miodownik, *Calculation of Phase Diagrams (CALPHAD): A Comprehensive Guide*, Pergamon Press, Pergamon, 1998
17. H. Ohtani and K. Ishida, Application of the CALPHAD Method to Material Design, *Thermochim. Acta*, 1998, **314**, p 69-77
18. J.C. Zhao, B.P. Bewlay, Jackson, and L.A. Peluso, *Structural Intermetallics*, TMS, Warrendale, PA, 2001, p 483
19. A.A. Nayeb-Hashemi and J.B. Clark, The Ag-Mg System, *Bulletin of Alloy phase diagrams*, 1984, **5**, p 348-354
20. S.F. Zemczuznyj, On the Alloys of Magnesium with Silver, *Z. Anorg. Allg. Chem.*, 1906, **49**, p 400-411
21. K.W. Andrews and W. Hume-Rothery, The Constitution of Silver-Magnesium Alloys in the Region 0-40 Atomic Precent Magnesium, *J. Inst. Met.*, 1943, **69**, p 485-493
22. R.J.M. Payne and J.L. Haughton, Alloys of Magnesium. Part IV the Constitution of the Magnesium-Rich Alloys of Mg and Ag, *J. Inst. Met.*, 1937, **60**, p 351-363
23. W. Hume-Rothery and E. Butchers, The Solubility of Silver and Gold in Solid Magnesium, *J. Inst. Met.*, 1937, **60**, p 345-350
24. N.V. Ageev and V.G. Kunezov, X-ray Study of Magnesium-silver Alloys, *Izv. Akad. nauk SSSR Otd. Nauk.*, 1937, p 289-309
25. H.R. Letner and S.S. Sidhu, An X-Ray Diffraction Study of the Silver-Magnesium Alloys System, *J. Appl. Phys.*, 1947, **18**, p 833-837
26. S. Goldsztaub and P. Michel, Preparation of Silver-Magnesium Alloys in Thin Layers by the Simultaneous Evaporation of these Constituents in Vacuum, *Compt. Rend.*, 1951, **232**, p 1843-1845
27. S. Nagashima, X-ray study of Guinier-preston zones fored in ager Magesium-rich, Magesium-silver alloys, *J. Jpn. Inst. Met.*, 1959, **23**, p 381-384
28. M.V. Prokofev, V.E. Kolesnichenko, and V.V. Karonik, Composition and Structure of Magnesium-silver Alloys with Composition near Mg3Ag, Izv. Akad. nauk. SSSR, *Neorg. Mater.*, 1985, **21**, p 1332-1334
29. V.E. Kolesnichenko, V.V. Karonik, S.N. Tsyganova, T.A. Kupriyanova, and L.N. Sysoeva, Phase Equilibria in the Mg-Ag System in the Eta Phase Region, *Izv. Akad. nauk. SSSR Neorg. Mater.*, 1988, **5**, p 186-191

30. M. Lim, J.E. Tibballs, and P.L. Rossiter, Thermodynamic Assessment of Ag-Mg Binary System, *Z. Metallkd.*, 1997, **88**, p 160-167
31. A. Gangulee and M.B. Bever, The Silver Rich Silid Solid Solutions in the System Ag-Mg, *Trans. Am. Inst. Min. Meta. Petro. Eng.*, 1968, **242**, p 272-278
32. M. Kawakami, A Further Investigation of the Heat of Mixture in Molten Metals, *Sci. Rep. Res. Inst. Tohoku Univ.*, 1930, **7**, p 351-364
33. J. Gran, M. Song, and D. Sichen, Acitivity of Magnesium in Liquid Ag-Mg Alloys, *CALPHAD*, 2012, **36**, p 89-93
34. S. Kachi, Thermodynamic Properties of Hume-Rothery Type Ag-Mg Alloy, *J. Jpn. Inst. Met.*, 1955, **19**, p 318-322
35. S. Kachi, Thermodynamic Properties of Hume-rothery Type Ag-Mg Alloy. (II). Activity of Mg in α Phase, and Free Energy, Entropy, etc. of α and β Phases, *J. Jpn. Inst. Met.*, 1955, **19**, p 378-382
36. P.M. Robinson and M.B. Bever, The Heat of Formation of the Intermetallic Compound Ag-Mg as a Function of Composition, *Trans. Metal. Soci. AIME*, 1964, **230**, p 1487-1488
37. A.K. Jena and M.B. Bever, On the Temperature Dependence of the Heat of Formation of the Compound Ag-Mg, *Trans. Metal. Soci. AIME*, 1968, **242**, p 2367-2369
38. W. Trzebiartowski and J. Terpilowski, Thermodynamic Properties of the Ag-Zn System and the Related beta-AgMg Phase, *Bull. Acad. Polon. Sci. Tech. Sco*, 1955, **3**, p 391-395
39. F. Weibke and H. Eggers, The Composition Diagram of the System Silver-Indium Z, *Anorg. Allg. Chem.*, 1935, **222**, p 145
40. W. Hume-rothert, G.W. Mabbott, K.M. Channel-evans, Philos. Trans. R. Soc. London A, 1934, **A233**, 1
41. E.A. Owen and E.W. Roberts, Factors Affecting the Limit of Solubility of Elements in Copper and Silver, *Phil. Magazin.*, 1939, **27**, p 294-327
42. V.E. Hellner, The Binary System Silver-Indium, *Z. Metallkd.*, 1951, **42**, p 17-19
43. A.N. Campbell, R. Wagemann, and R.B. Ferguson, The Silver-Indium System: Thermal Analysis, Photomicrography, Electron Microprobe, and X-ray Powder Diffraction Results, *Can. J. Chem.*, 1970, **48**, p 1703-1715
44. O. Uemura and I. Satow, Order-Disorder Transition of Silver-Indium (Ag3In) Alloy, *Trans. Jpn. Inst. Met.*, 1973, **14**, p 199-201
45. T. Satow, O. Uemura, and S. Yamakawa, X-ray Diffraction and Electrical Resistivity Study of Silver-Indium (Ag2In) and High Temperature Ag3In Phases, *Trans. Jpn. Inst. Met.*, 1973, **15**, p 253-255
46. Barren, Ag-In (Silver-Indium), *Phase Diagrams of Indium Alloys and Their Engineering Applications*, H.O.C.E.T. White, Ed., ASM international, Novelty, 1992, p 15-19
47. Z. Moser, W. Gasior, J. Pstrus, W. Zakulski, I. Ohnuma, X.J. Liu, Y. Inohana, and K. Ishida, Studies of the Ag-In Phase Diagram and Surface Tension Measurements, *J. Electron. Mater.*, 2001, **30**, p 1120-1128
48. D. Jendrzejczyk and K. Fitzner, Thermodynamic Properties of Liquid Silver-Indium Alloys Determined From EMF Measurements, *Thermochim. Acta*, 2005, **433**, p 66-71
49. O.J. Kleppa, Heat of Formation of Solid and Liquid Alloys in the Systems Ag-Cd, Ag-In and Ag-Sb at 450 °C, *J. Phys. Chem.*, 1956, **60**, p 846-852
50. E. Prezdziecka-Mycielska, J. Terpilowski, and K. Strozecka, Thermodynamic Properties of Liquid Metallic Solutions. XI. The Ag-In System, Archi, *Hutnictwa*, 1963, **2**, p 85-101
51. T. Nozaki, M. Shimoji, and K. Niwa, Thermodynamic Properties of Ag-In Liquid Phase, *Trans. Jpn. Inst. Met.*, 1966, **30**, p 7-10
52. R. Beja, Enthalpy of Mixing of Liquid Silver-gallium Alloys at 500 °C, *C. R. Acad. Sci.*, 1968, **267**, p 123-126
53. K. Itagaki and A. Yazawa, Measurements of Heats of Mixing in Liquid Ag Binary Alloys, *Trans. Jpn. Inst. Met.*, 1968, **32**, p 1294-1300
54. C.B. Alcock, R. Sridhar, R.C. Svedberg, A Mass Spectrometric Study of the Binary Liquid Alloys, Ag-In and Cu-Sn, Acta Metall. Mater., 1969, **17**
55. G.J. Qi, H. Mitsuhisa, and A. Takeshi, Thermodynamic Study of Liquid Silver-Indium and Silver-Gallium Alloys with a Knudsen Cell-Mass Spectrometer, *Mater. Trans., JIM*, 1989, **30**, p 575-582
56. K. Kameda, Y. Yoshida, and S. Sakairi, Activities of Liquid Silver-Indium Alloys by EMF Measurements Using Zirconia Solid and Fused Salt Electrolytes, *Trans. Jpn. Inst. Met.*, 1981, **45**, p 614-620
57. R. Castanet, Y. Claire, and M. Laffitte, Thermodynamic Properties of Liquid Ag-In Solutions, *J. Chim. Phys.Physico-chim.Biolog.*, 1970, **67**, p 789-793
58. L.R. Orr and R. Hultgren, Heat Formation of α-Phase Silver-Indium Alloys, *J. Phys. Chem.*, 1961, **65**, p 378-380
59. D.B. Masson and S.S. Pradhan, Measurement of Vapor Pressure of Indium over a Ag-In Using Atomic Absorption, *Metall. Mater. Trans. A*, 1973, **4**, p 991-995
60. C.T. Heycock and F.H. Neville, The Molecular Weights of Metals When in Solution, *J. Chem. Soc.*, 1890, **57**, p 373-393
61. C.T. Heycock and F.H. Neville, The Freezing Point of Triple Alloys, *J. Chem. Soc.*, 1894, **65**, p 65-76
62. C.T. Heycock and F.H. Neville, Complete Freezing Point Curves of Binary Alloys Containing Silver or Copper, *Phil. Trans. Roy. Soc. A*, 1897, **189**, p 25-69
63. G.J. Peternko, On the Alloying of Silver with Lead and Tin, *Z. Anorg. Allg. Chem.*, 1907, **56**, p 20-22
64. N. Puschin, Das potential die chemiusche konstitution der metalllegierunge, *Z. Anorg. Allg. Chem.*, 1908, **56**, p 1-45
65. A.J. Murphy, The Constitution of the Alloys of Silver and Tin, *J. Inst. Met.*, 1926, **35**, p 107-129
66. W. Hume-Rothery, G.W. Mabbot, and K.M. Channel-Evans, The Freezing Points, Melting Points and Solid Solubility Limits of the Alloys of Silver and Copper with the Elements of the Sub-Groups, *Phil. Trans. Roy. Soc. A*, 1934, **233**, p 1-97
67. W. Hume-Rothery and P.W. Reynolds, The Accurate Determination of the Freezing Points of Alloys and a Study of Valency Effects in Certain Alloys of Silver, *Proc. R. Soc. London A*, 1937, **160**, p 282-303
68. D. Hanson, E.J. Stand, and H. Syevens, Some Properties of tin Containing Small Amounts of Silver, Iron, Nickel or Copper, *J. Inst. Met.*, 1934, **55**, p 115-133
69. A.E. Owen and E.W. Roberts, Facts Affecting the Limit of Solubility of Elements in Copper and Silver, *Philos. Mag.*, 1939, **27**, p 294-327
70. M.M. Umansky, Diagram of the Alloy Silver-Tin, *Zhurnal Fiz. Khim.*, 1940, **14**, p 846-849
71. F. Vnuk, M.H. Ainsley, and R.W. Smith, The Solid Solubility of Silver, Gold and Zinc in Metallic Tin, *J. Mater. Sci.*, 1981, **16**, p 1171-1176
72. I. Karakaya, W.T. Thompson, The Ag-Sn system, *Bull. Alloy Phase Diag.*, 1987, **8**, p 340-347
73. R.O. Frantik and H.J. McDaonald, Thermodynamic Study of the Tin-Silver System, *Trans. Electrochem. Soc.*, 1945, **88**, p 253-262
74. J.A. Yanko, A.E. Drake, and F. Hovorka, Thermodynamic Studies of Dilute Solutions in Molten Binary Alloys, *Trans. Electrochem. Soc.*, 1946, **89**, p 357-372

75. O.J. Kleppa, A Calorimetric Investigation of the System Ag-Sn at 450 °C, *Acta Metall.*, 1955, **3**, p 255-259
76. T. Nozaki, M. Shimoji, and K. Niwa, Thermodynamic Properties of Ag-Sn and Ag-Sb Liquid Alloys, *Beri. Bun. Gesellscha.*, 1966, **70**, p 207-214
77. R.B. Elliott and J.F. Lemons, Activites of Molten tin Alloys from EMF Measurements, *J. Electrochem. Soc.*, 1967, **114**, p 935-937
78. R. Castanet and M. Laffitte, Enthalpie de formation a 1280 K d'alliages liquides argent-etain et argent-germanium, *C. R. Acad. Sci. Paris. C*, 1968, **267**, p 204-206
79. P.J.R. Chowdhury and A. Ghosh, Thermodynamic Measurements in Liquid Sn-Ag Alloys, *Metall. Trans.*, 1971, **2**, p 2171-2174
80. K. Okajima and H. Sakao, Tie Measurements on the Activities of the Ag-Sb, Ag-Pb and Ag-Sn Molten Alloys, *Trans. JIM*, 1974, **15**, p 52-56
81. M. Iwase, M.O. Yasuda, and S.I. Miki, A Thermodynamic Study of Liquid Ag-Sn Alloys by Means of Solid-Oxide Galvanic Cell, *Trans. JIM*, 1978, **19**, p 654-660
82. K. Kameda, Y. Yoshida, and S. Sakairi, Thermodynamic Properties of Liquid Ag-Sn Alloys, *J. Jpn. Inst. Met.*, 1980, **44**, p 858-863
83. H. Flandorfer, U. Saeed, C. Luef, A. Sabbar, and H. Ipser, Interfaces in Lead-Free Solder Alloys: Enthalpy of Formation of Binary Ag-Sn, Cu-Sn and Ni-Sn Intermetallic Compounds, *Thermochim. Acta*, 2007, **459**, p 34-39
84. J. Rakotomavo, M. Gaune-Escard, J.P. Bros, and P. Gaune, Enthalpies of Formation at 1373 K of the Liquid Alloys Ag-Au, Ag-Sn, and A-Au-Sn, *Ber. Bunssenges.*, 1974, **88**, p 663-670
85. G.H. Laurie, A.H. Morris, and J.N. Pratt, Electromotive Force and Calorimetric Studies of Thermodynamic Properties of Solid and Liquid Ag-Sn Alloys, *Trans. Metall. AIME*, 1966, **236**, p 1390-1395
86. T. Yamaji and E. Kato, Mass Spectrometric Study of the Thermodynamic Properties of the Ag-Sn System, *Metall. Mater. Trans. B*, 1972, **3**, p 1002-1004
87. V.E. Kolesnichenko, M.A. Komapoba, and B.B. Kapohhk, Study of the Magnesium-Silver-Indium Phase Diagram, Izv. Akad. nauk SSSR, *Neorg. Mater.*, 1982, **5**, p 225-229
88. G.V. Raynor and B.R.T. Frost, The System Ag-Mg-Sn with Reference to the Theory of Ternary Alloys, *J. Inst. Met.*, 1949, **75**, p 777-808
89. V.V. Karonik, V.E. Kolesnichenko, A.A. Shepelev, G.I. Kandyba, Magnesium-Silver-Tin Phase Diagram, Metalloved. Splavov na Osnove Tsv. Met. M., 1983, p 78-84
90. T.M. Korhonen and J.K. Kivilahti, Thermodynamics of the Sn-In-Ag Solder System, *J. Electron. Mater.*, 1998, **27**, p 149-158
91. X.J. Liu, Y. Inohana, Y. Takaku, I. Ohnuma, R. Kainuma, K. Ishida, Z. Moser, W. Gasior, and J. Pstrus, Experimental Determination and Thermodynamic Calculation of the Phase Equilibira and Surface Tension in the Sn-Ag-In System, *J. Electron. Mater.*, 2002, **31**, p 1139-1151
92. G. Vassilev, E.S. Dobrev, and J.C. Tedenac, Experimental Study of the Ag-Sn-In Phase Diagram, *J. Alloy. Comp.*, 2005, **399**, p 118-125
93. T. Miki, N. Ogawa, T. Nagasaka, and M. Hino, Activity Measurement of the Constituents in Molten Sn-Ag-In and Sn-Zn-Mg ternary Lead Free Solder Alloys by Mass Spectrometry, *Metall. Mater. Proc. Prin. Tech.*, 2003, **1**, p 405-415
94. B. Gather, P. Schroeter, and R. Blachnik, Heats of Mixing in the Silver-Indium-Tin, Silver-Tin-Antimony, Silver-Indium-Antimony, and Indium-Lead-Antimony Ternary Systems, *Z. Metallkd.*, 1987, **78**, p 280-285
95. I.-H. Jung, D.H. Kang, W.J. Park, N.J. Kim, and S.H. Ahn, Thermodynamic Modeling of the Mg-Si-Sn system, *CALPHAD*, 2007, **31**, p 192-200
96. P. Ghosh, M.D. Mezbahul-Islam, and M. Medraj, Critical Assessment and Thermodynamic Modeling of Mg-Zn, *Mg-Sn, Sn-Zn and Mg-Sn-Zn system, CALPHAD*, 2012, **36**, p 28-43
97. J. Wang, I.H. Jung, P. Chartrand, and M. Medraj, Experimental and Thermodynamic Studying on Mg-Sn-In-Zn System, *J. Alloy. Comp.*, 2014, **588**, p 75-95
98. S.C. Oh, J.H. Shim, B.J. Lee, and D.N. Lee, Thermodynamic Study on the Ag-Sb-Sn System, *J. Alloy. Comp.*, 1996, **238**, p 155-166
99. F. Meng, J. Wang, L. Liu, and Z. Jin, Thermodynamic Modeling of the Mg-Sn-Zn Ternary System, *J. Alloy. Comp.*, 2010, **508**, p 570-581
100. A.T. Dinsdale, SGTE Data for Pure Elements, *CALPHAD*, 1991, **15**, p 317-425
101. C.W. Bale, P. Chartrand, S.A. Degterov, G. Eriksson, K. Hack, R. Ben Mahfoud, J. Melancon, A.D. Pelton, and S. Petersen, Factage Thermochemical Software and Databases, *CALPHAD*, 2002, **26**, p 189-228
102. H. Kopp, Investigations of the Specific Heat of Solid Bodies, *Phil. Trans. Roy. Soc. A*, 1865, **155**, p 71-202
103. M. Hillert, The Compound Energy Formalism, *J. Alloy. Comp.*, 2001, **320**, p 161-176
104. N. Dupin and I. Ansara, On the Sublattice Formalism Applied to the B2 Phase, *Z. Metallkd.*, 1999, **90**, p 76-85
105. A.D. Pelton and P. Chartrand, The Modified Quasi-Chemical Model: Part II. Multicomponent Solutions, *Metall. Mater. Trans. A*, 2001, **32**, p 1355-1360
106. A.D. Pelton, S.A. Degterov, G. Eriksson, C. Robelin, and Y. Dessureault, The Modified Quasichemical Model I-Binary Solutions, *Metall. Mater. Trans. B*, 2000, **31**, p 651-659
107. A.D. Pelton, A General "geometric" Thermodynamic Model for Multicomponent Solutions, *CALPHAD*, 2001, **25**, p 319-328
108. D. Zivkovic, A. Milosavljevic, A. Mitovski, and B. Marjanovic, Comparative Thermodynamic Study and Characterization of Ternary Ag-In-Sn Alloys, *J. Therm. Anal. Calorim.*, 2007, **89**, p 137-142
109. V.E. Kolesnichenko, I.M. Khatsernov, and V.V. Karonik, Phase Composition of Magnesium-Silver-Indium-Tin Alloys in the Magnesium-Rich Region, *Izv. Akadem. nauk. SSSR Metall.*, 1989, **2**, p 219-221
110. J. Wang, N.H. Miao, P. Chartrand, and I.-H. Jung, Thermodynamic Evaluation and Optimization of the (Na+X) Binary Systems (X=Ag, Ca, as Part of a Wider Thermodynamic Database Development Project for the Mg-X (X: Ag, Ca, In, Li, Na, Sn, Sr and Zn) Multi-Component System,*J. Chem. Thermodyn.*, 2013, **66**, p 22-33